DOE/ER/52159--2

DE91 007912



# Neutral Transport and Helium Pumping of ITER

Annual Progress Report

for period January 15, 1990 - January 14, 1991

David N. Ruzic

University of Illinois
Urbana, Illinois 61801

August 1990

Prepared for

The U.S. Department of Energy
Agreement No. DE-FG02-89ER52159

**Abstract**

A 2-D Monte-Carlo simulation of the neutral atom densities in the divertor, divertor throat and pump duct of ITER was made using the DEGAS code. Plasma conditions in the scrape-off layer and region near the separatrix were modeled using the B2 plasma transport code. Wall reflection coefficients including the effect of realistic surface roughness were determined by using the fractal TRIM code. The DEGAS and B2 coupling was iterated until a consistent recycling was predicted. Results were obtained for a helium and a deuterium/tritium mixture on 7 different ITER divertor throat geometries for both the physics phase reference base case and a technology phase case. Recycling, pumping efficiency ratios, temperatures and densities vary markedly.

The geometry with a larger structure on the midplane-side of the throat opening closing the divertor throat (a "big nose") and a divertor plate which maintains a steep slope well into the throat ("no lip") removed helium 1.5 times better than the reference geometry for the physics phase case and 2.2 times better for the technology phase case. At the same time the helium to hydrogen pumping ratio shows a factor of 2.34 ± .41 enhancement over the ratio of helium to hydrogen incident on the divertor plate in the physics phase and an improvement of 1.61 ± .31 in the technology phase. If the helium flux profile on the divertor plate is moved outward by 20 cm with respect to the D/T flux profile for this particular geometry, the enhancement increases to 4.36 ± .90 in the physics phase and 5.10 ± .92 in the technology phase.

# Table of Contents

## I. Introduction

The International Thermonuclear Experimental Reactor (ITER) tokamak is being designed to achieve long-pulse ignited operation.[1] To achieve those goals, steady state removal of helium ash must be sufficient to maintain a core helium concentration of less than 10%[2] while maintaining a realistic pumping system and minimizing the tritium inventory. This contract investigates the effect of the divertor shape and pump duct geometry on deuterium/tritium and helium exhaust.

Two computer codes are coupled in this work. The B2 transport code[3] is a 2-D fluid model which solves the first three coupled moment equations: continuity, momentum balance, and energy balance. Thermal conductivity, diffusivity, viscosity, etc. are taken from recommendations based on a tokamak database.[4] The magnetic flux surfaces for the outboard portion of the double-null ITER configuration are taken as the grid boundaries. The source rate and location for new ions from the divertor plate is determined by specifying a local recycling coefficient along the plate boundary. The B2 code iterates until a self-consistent solution is obtained.

The DEGAS code[5] is a 3-D Monte-Carlo multi-species neutral transport code which contains extensive atomic physics including charge exchange, electron and ion impact ionizations, molecular dissociations etc. Energy and angle-resolved wall reflection coefficients include effects of surface roughness and are taken from fractal TRIM.[6,7] The source rate of neutral atoms comes from the flux of ions to the divertor plate. Neutral atoms are followed until they become ionized or exit the simulation geometry.

The B2 and DEGAS codes were iterated with a 50-50 D/T plasma until their respective boundary conditions at the divertor plate matched. Then helium was included in DEGAS and several geometries of the divertor throat were simulated. The next section explains the details of coupling the models and shows their inputs. The resultant neutral densities and recycling coefficients show significant variation as a function of geometry.

## II. Models

Input parameters to the B2 code are shown in table 1, below. Both cases were for ITER double-null ignited plasmas.

**Table 1** Input parameters for the B2 code

| | Physics (A1) | Technology (B63) |
|---|---|---|
| ohmic heating + auxiliary + alpha power | 218 MW | 263 MW |
| power entering inner and outer scrape-off-layer | 116 MW | 187 MW |
| volume averaged electron density | 1.22e20 $m^{-3}$ | 0.64e20 $m^{-3}$ |
| electron density at the midplane separatrix | 0.349e20 | 0.183e20 |
| $Z_{eff}$ core | 1.66 | 2.20 |
| $Z_{eff}$ midplane | 1.53 | 1.96 |
| plasma current | 22 MA | 18.9 MA |

The B2 geometry is shown in the upper half of figure 1. The X-point to divertor strike-point distance is 1.5 m. Though the B2 code is not yet capable of directly simulating a tilted divertor plate, a tilt of 15 degrees is included in the calculations.

The output of the B2 code includes plasma density, electron and ion temperatures in each zone. These values for the lower 24 horizontal by 16 vertical B2 zones were mapped onto the appropriate 24 by 16 zones of the DEGAS geometry (lower half of figure 1). The distance between the X-point and strike point in the DEGAS simulation was also 1.5 m. The DEGAS geometry was taken directly from the current engineering drawings of the ITER divertor throat. The volume of the individual zones were not preserved during the mapping, but the density, flux and alignment of the zones with the field were maintained. Figure 2 shows contour plots of the B2 temperature and density outputs as they appear in the realistic (DEGAS) geometry for both the physics and technology phases.

In addition to the 2-D plasma profiles, DEGAS needs the ion flux distribution along the divertor plate to act as the neutral source. This is obtained from the temperature and densities of the boundary zones in the B2 simulation and is shown in figure 3 for the physics phase.

Also shown in figure 3 is the local recycling coefficient used in the B2 code to match the DEGAS results. Several iterations were performed until the net current of atoms across the separatrix in B2 equalled the net loss of atoms to the pump in DEGAS. This iteration was done in two parts. The net loss of particles in B2 is obtained by integrating the flux and the recycling coefficient in figure 3. For the physics phase case, the integrated recycling coefficient equals 0.990. That is, for every 1000 particles that hit the divertor plate, 10 are removed from the B2 simulation. The integrated recycling coefficient equals 0.9965 for the technology phase case. The net loss of particles in DEGAS is obtained by comparing the number of atoms that exit the simulation through the pump compared to the number that are initiated on the divertor plate.

For this comparison to be valid, 3-dimensional effects must be included. For the B2 code, toroidal symmetry is a valid assumption. However, pump ducts only cover 25% of the ITER design. Further, conductance per unit width through an infinitely wide rectangular duct is greater than one with side walls. For the dimensions of ITER this effect should reduce the pumping efficiency of the 2-D (i.e. infinite in the third dimension) simulation by 15%.[8] The as-simulated DEGAS recycling coefficient for the physics phase reference case was 0.952. Of 1000 initiated flights, 48 left through the pump openings. If this number is first corrected for 3-D conductance and then for toroidal duct coverage it becomes 0.9898 $\pm$ 0.0014. That is, for every 1000 atoms that strike the plate, 10.2 $\pm$ 1.4 would leave the device. The corrected DEGAS recycling coefficient for the technology phase is 0.9962 $\pm$ 0.0005.

Once a match with the B2 code was obtained, seven geometries were simulated. Figure 4 shows the variations and the two prominent features. The reference case (shown with solid lines), has both a "nose" at the top of the duct entrance and a curved "lip" as part of the divertor plate. Simulations were performed varying the size and combination of these features. All simulations had a pump reflectance of 87.5%. Only 2 of the 16 sections at the end of the duct allowed particles to exit. The other pump boundaries as well as the plasma boundaries were treated as mirrors to all particles. The walls were made of carbon. Any non-reflected atom left the wall as a molecule at the wall temperature. This was taken to be 450 C in the pump duct and higher on the plate, but the exact value had little effect other than determining the average energy of the exiting D/T molecules.

$He^{++}$ was added to the DEGAS simulation at the same temperature as the $D/T^{+}$. The density was adjusted to give a flux profile on the divertor plate equal to 0.1 times the D/T profile. For most of the cases presented, the flux profiles were not offset from one another. Though charge exchange between D/T and He is included, neutral-neutral scattering is not. Since neutral atom scattering is very forward peaked[9] the exclusion of this process is not expected to have a large influence on the results. Note that a D/T atom is a hydrogenic species with a mass of 2.5 amu. A D/T molecule has a mass of 5.0 amu.

## III. Results

The reference geometry was run on the MFECC Cray 2 "b" machine. A DEGAS run of 1000 D/T flights and 1000 He flights took a total of approximately 200 cpu minutes for the physics phase cases and runs of 2000 D/T flights and 2000 He flights took a total of approximately 130 minutes for the technology phase cases. The length of the simulation was due to the large geometrical size and paucity of exits. The technology phase cases ran faster because the plasma in the divertor region was hotter and ionization of the neutral occurred more quickly. Figure 5 shows contour plots of the D/T atom density and temperature, D/T molecular density and the He atom density and temperature for both phases. The only regions of appreciable atomic temperature is where the density falls markedly due to the presence of the plasma. The spatial variation of the molecules in the pump duct is quite uniform.

Figure 6 shows the effect of varying geometry on the helium exhaust. Within each phase the number of helium atoms and current to the divertor plate was the same for each geometry. The results are normalized to the reference geometry. The current leaving through the pump duct opening varies markedly with geometry for both phases. The presence of a bigger nose increases the helium conductance by preventing slowed helium atoms from wandering back to the plasma to become reionized. The absence of a lip also increases the helium pumping. More ions can be reflected (as atoms) directly toward the duct opening.

Actual pumping also depends on the energy of the exiting species, though many more bounces with the walls may occur before the actual pump is encountered. Table 2, below, compares the average energy of the exiting helium for all geometries and cases.

**Table 2** Average energy of exiting helium

| Geometry | | Physics | Technology |
|---|---|---|---|
| nose | lip | | |
| no | ref. | 0.82 eV | 1.1 eV |
| ref. | ref. | 1.3 | 2.5 |
| big | ref. | 0.65 | 2.6 |
| ref. | small | 1.5 | 1.2 |
| no | no | 1.1 | 1.3 |
| ref. | no | 1.4 | 1.9 |
| big | no | 1.4 | 2.3 |

Figure 7 looks at the geometric effects on the exiting D/T currents. Again the initial current to the divertor plate is the same for each geometry within a given phase and the results are normalized to the reference geometry. The effects on the D/T currents are not as large as the geometric effects on the helium atoms since D/T exists as atoms and molecules. Figure 8 shows the percentage of the exiting D/T current which is in the atomic state. Figure 9 shows the average energy of the atoms. The average energy of the molecules did not vary much. The no lip cases had a slightly higher molecular temperature, 0.047 eV instead of 0.039 eV, since the divertor plate itself was warmer than the walls of the pump duct.

Table 3 summarizes the results of varying geometry on the average densities near the end of the pump duct. The standard error for the atomic D/T quantities is roughly 30%. The standard error for the molecular, $(D/T)_2$, quantities is roughly 15%, and the standard error for the He quantities is roughly 10%.

**Table 3** Average densities along pump duct

| Geometry | | Physics av. density ($10^{14}cm^{-3}$) | | | Technology av. density ($10^{14}cm^{-3}$) | | |
|---|---|---|---|---|---|---|---|
| nose | lip | D/T | $(D/T)_2$ | He | D/T | $(D/T)_2$ | He |
| no | ref. | 0.20 | 8.5 | 2.0 | 0.05 | 1.5 | .23 |
| ref. | ref. | 0.23 | 11.2 | 2.2 | 0.06 | 1.9 | .27 |
| big | ref. | 0.08 | 10.9 | 3.6 | 0.03 | 2.2 | .51 |
| ref. | small | 0.17 | 11.4 | 2.4 | 0.05 | 1.9 | .27 |
| no | no | 0.34 | 12.0 | 2.2 | 0.09 | 1.8 | .37 |
| ref. | no | 0.30 | 12.4 | 2.4 | 0.05 | 1.8 | .53 |
| big | no | 0.21 | 14.6 | 3.4 | 0.09 | 1.8 | .33 |

Table 4 contains the as-simulated recycling coefficients, $R_{D/T}$ and $R_{He}$. This recycling coefficient, R, is defined as:

$$R = 1 - \frac{\text{number going out pump duct}}{\text{number of ions striking divertor plate}}$$

**Table 4** Recycling coefficients

| Geometry nose | Geometry lip | Physics $R_{D/T}$ | Physics $R_{He}$ | Technology $R_{D/T}$ | Technology $R_{He}$ |
|---|---|---|---|---|---|
| no | ref. | .962 Γ.005 | .947 Γ.007 | .987 Γ.002 | .981 Γ.003 |
| ref. | ref. | .952 Γ.007 | .936 Γ.007 | .982 Γ.002 | .985 Γ.003 |
| big | ref. | .969 Γ.007 | .917 Γ.008 | .984 Γ.003 | .978 Γ.003 |
| ref. | small | .972 Γ.005 | .933 Γ.008 | .987 Γ.003 | .979 Γ.003 |
| no | no | .953 Γ.006 | .923 Γ.008 | .985 Γ.003 | .978 Γ.003 |
| ref. | no | .948 Γ.007 | .927 Γ.008 | .982 Γ.003 | .969 Γ.004 |
| big | no | .959 Γ.006 | .904 Γ.009 | .975 Γ.004 | .960 Γ.004 |

Table 5 show the helium pumping enhancement factor. This factor, F, is defined as:

$$F = \frac{1 - R_{He}}{1 - R_{D/T}}$$

and represents the enhancement of helium pumping over D/T pumping for the same number of particles per unit time striking the divertor plate.

**Table 5** Helium enhancement factor

| Geometry nose | lip | Physics F | Technology F |
|---|---|---|---|
| no | ref. | 1.40 ± .27 | 1.39 ± .31 |
| ref. | ref. | 1.33 ± .24 | .84 ± .16 |
| big | ref. | 2.67 ± .53 | 1.34 ± .29 |
| ref. | small | 2.39 ± .50 | 1.64 ± .40 |
| no | no | 1.64 ± .28 | 1.48 ± .35 |
| ref. | no | 1.40 ± .23 | 1.75 ± .39 |
| big | no | 2.34 ± .41 | 1.61 ± .31 |

Table 5 shows that helium is almost always preferentially pumped over D/T. This is largely due to the higher reflection coefficient of He on C at low energies. D/T are more likely to stick to walls and come off as slow molecules. The presence of a nose dramatically increases the chance of He exiting. The total absence of a lip improves the pumping of all species.

The flux profile of $He^{++}$ on the divertor plate was shifted along the plate toward the duct by 20 cm for four geometries in the physics phase and two geometries for the technology phase. The results are shown in table 6. Moving the flux outward by this amount markedly decreases $R_{He}$ and increases F for all of the geometries tested.

## IV. Conclusions

The geometry with a big nose and no lip is the best at pumping helium and enhancing the pumping of helium over D/T of the geometries tested for both the physics and technology phases of ITER. Shifting the flux of helium ions outward on the divertor plate with respect to the D/T ions significantly enhances the helium pumping. Further modeling and experimental work should be pursued in edge helium transport.

**Table 6** Effect of shifting the helium flux profile

| Geometry nose | Geometry lip | shift (cm) | $n_{He}$ ($cm^{-3}$) x $10^{14}$ | av E (eV) | $R_{He}$ | F |
|---|---|---|---|---|---|---|
| **Physics Phase:** | | | | | | |
| ref. | ref. | none | 2.2 | 1.3 | .936 ± .007 | 1.33 ± .24 |
| | | +20 | 4.3 | 1.1 | .851 ± .016 | 3.10 ± .54 |
| big | ref. | none | 3.6 | .65 | .917 ± .008 | 2.67 ± .53 |
| | | +20 | 5.6 | .48 | .865 ± .015 | 4.36 ± .90 |
| ref. | no | none | 2.4 | 1.4 | .927 ± .006 | 1.40 ± .23 |
| | | +20 | 3.8 | 1.4 | .853 ± .016 | 2.83 ± .47 |
| big | no | none | 3.4 | 1.4 | .904 ± .009 | 2.34 ± .41 |
| | | +20 | 5.4 | .73 | .789 ± .019 | 5.15 ± .88 |
| **Technology Phase:** | | | | | | |
| ref. | ref. | none | 0.27 | 2.8 | .985 ± .003 | 0.84 ± .16 |
| | | +20 | 0.77 | 1.2 | .940 ± .005 | 3.37 ± .58 |
| big | no | none | 0.53 | 1.9 | .960 ± .004 | 1.61 ± .31 |
| | | +20 | 1.6 | 1.9 | .875 ± .010 | 5.10 ± .92 |

## V. Future Work

The geometry of ITER has not yet been fully specified. More geometric shapes, consistent with the engineering realities must be modeled. These runs should be fully coupled to well-developed helium profiles and treat the albedo of the pump in more detail. A full 3-D simulation is possible, since pumping will not be toroidally symmetric.

In addition DEGAS can be used to model expected diagnostic signals in the divertor region. Charge-exchange, spectroscopic H-aplha signals, and bolometric signals can be simulated to check diagnostic placement and sensitivity.

## VI. Acknowledgements

This work was performed under DOE contracts: DOE-DEFG-02-89-ER52159. Able assistance was provided to DNR by Daniel Juliano, undergraduate physics major, University of Illinois.

## VII. References

[1] International Thermonuclear Experimental Reactor (ITER), Establishment of ITER: Relevant Documents, IAEA Vienna (1988).

[2] M.H. Redi, S.A. Cohen, 9th International Conference on Plasma Surface Interactions, Bournesmouth UK, May 1990.

[3] B. Braams, Eur. Conf. on Controlled Fusion and Plasma Physics, Part II, Budapest (1985) 480.

[4] Summary Report for the January March Joint Work Session 1990, ITER-IL-Ph-5-0-42.

[5] D.B. Heifetz et. al. J. Comp. Phys. **46** (1982) 309.

[6] D.N. Ruzic and H.K. Chiu, J. Nucl. Mater. **162-164** (1989) 904.

[7] D.N. Ruzic, Nucl. Instrum. and Met. B47 (1990) 118.

[8] S. Dushman, "Scientific Foundations of Vacuum Technique", Wiley, New York, (1949).

[9] D.N. Ruzic, PhD dissertation, Princeton University, 1984.

## VIII. Figure Captions

**Figure 1.** B2 simulation (upper portion) and DEGAS simulation (lower portion) geometries. The lower 24 horizontal by 16 vertical zones of the B2 simulation were mapped onto 24 by 16 zones of the DEGAS simulation. The X-

point to strike point distance was 1.5 m for both simulations.

**Figure 2.** B2 outputs mapped onto DEGAS zones for the physics phase (a) electron density, (b) electron temperature, and (c) ion temperature and the technology phase (d) electron density, (e) electron temperature, and (f) ion temperature. The contour plots are logarithmic for density in $cm^{-3}$. The numbers on the plots are the exponents. Temperature contour plots are in eV.

**Figure 3.** Flux to the divertor plate and B2 recycling profile needed to match the recycling in the coupled code for the physics phase case. The separatrix is at 0 cm on the x-axis.

**Figure 4.** Divertor and pump duct geometries used in this paper. The albedo of the pump was simulated by having only 12.5% of the pump duct area open on the right hand side of this figure.

**Figure 5.** DEGAS outputs for the reference geometry. Physics phase: (a) Density of D/T atoms ($cm^{-3}$). (b) Temperature of D/T atoms (eV). (c) Density of molecular D/T ($cm^{-3}$). (d) Density of He atoms ($cm^{-3}$). (e) Temperature of He atoms (eV). Technology phase: (f) Density of D/T atoms ($cm^{-3}$). (g) Temperature of D/T atoms (eV). (h) Density of

molecular D/T ($cm^{-3}$). (i) Density of He atoms ($cm^{-3}$). (j) Temperature of He atoms (eV). The contour plots are logarithmic for density in $cm^{-3}$. The numbers on the plots are the exponents.

**Figure 6.** Helium current exiting through the pump duct as a function of geometry. Results are normalized to the reference geometry. Within a given operation phase (physics or technology), the current to the plate is the same for each geometry.

**Figure 7.** D/T current exiting through the pump duct as a function of geometry. Results are normalized to the reference geometry. Within a given operation phase (physics or technology), the current to the plate is the same for each geometry. The D/T current is a combination of molecules and atoms indicating the number of D/T nuclei exiting the simulation through the pump duct.

**Figure 8.** Percentage of the D/T current that exits as atoms as a function of geometry.

**Figure 9.** Average energy of the exiting D/T atoms as a function of energy. The standard error in atom energies is quite high, approximately 50%, especially for the low atomic percent cases.

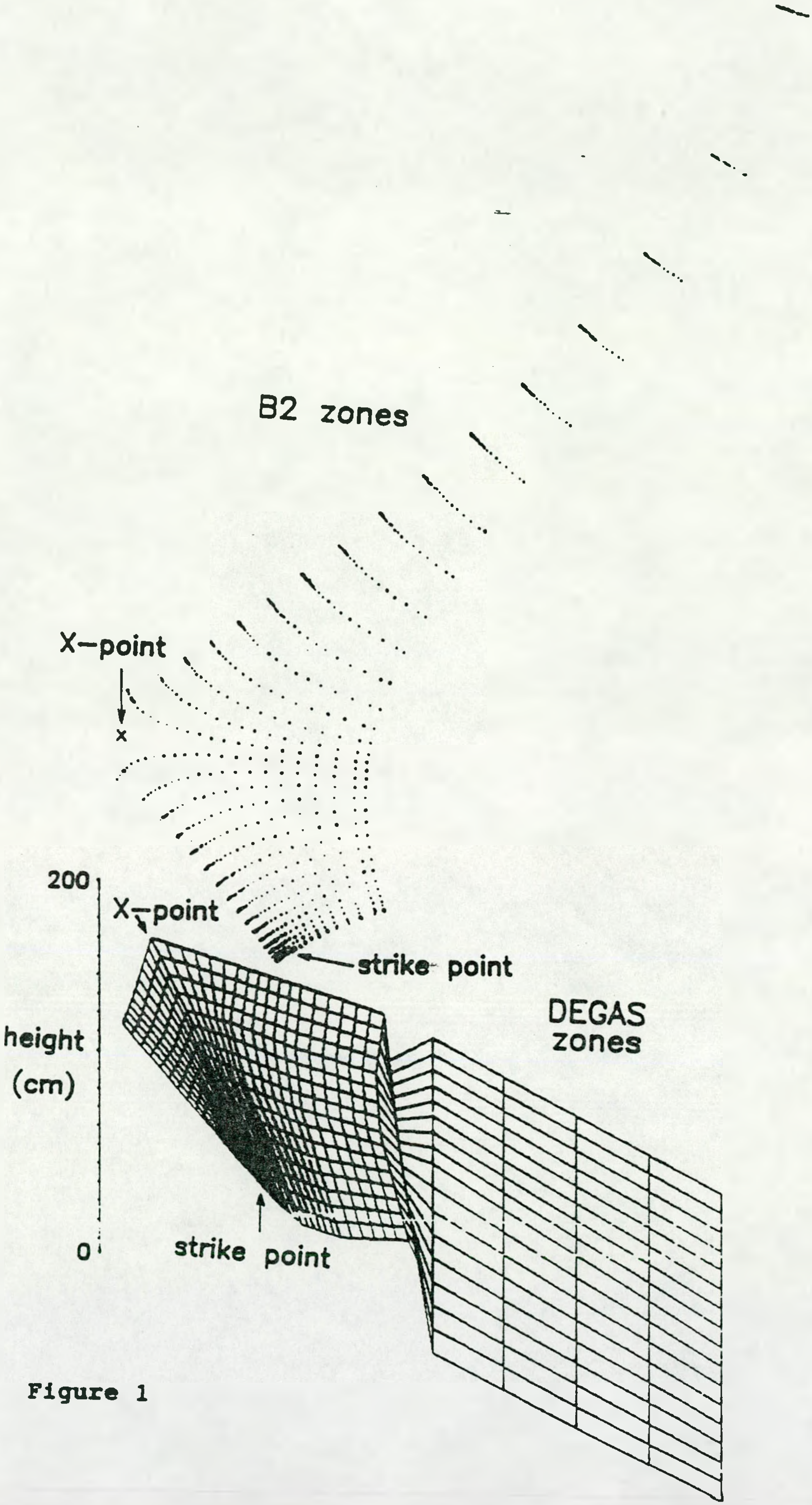
B2 zones
X–point
x
200
X–point
strike point
height
(cm)
DEGAS
zones
0
strike point

Figure 1

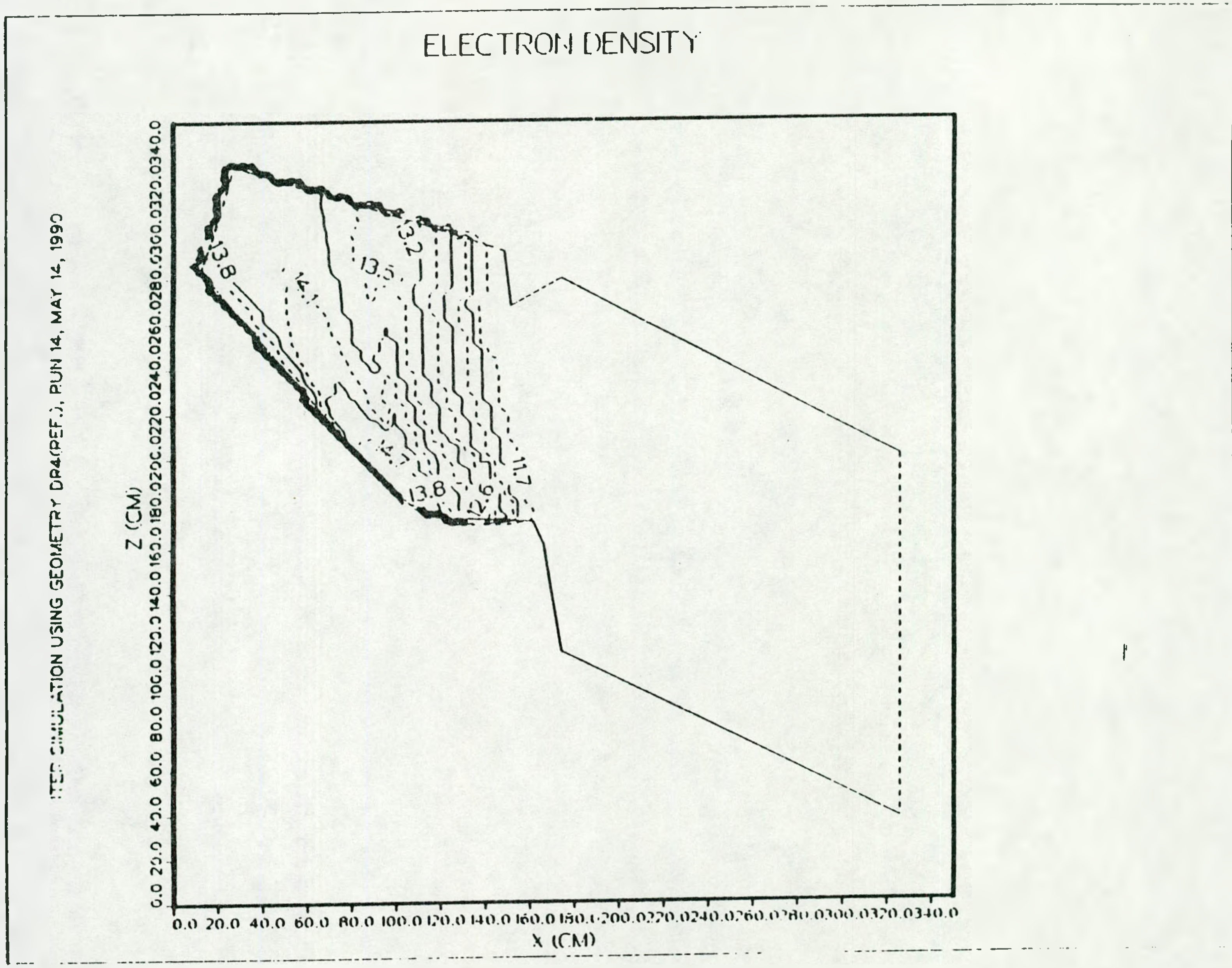
ELECTRON DENSITY
SIMULATION USING GEOMETRY DR4(REF.), RUN 14, MAY 14, 1990
Z (CM)
X (CM)
13.8
13.2
13.5
14.1
14.7
11.7

Figure 2 a

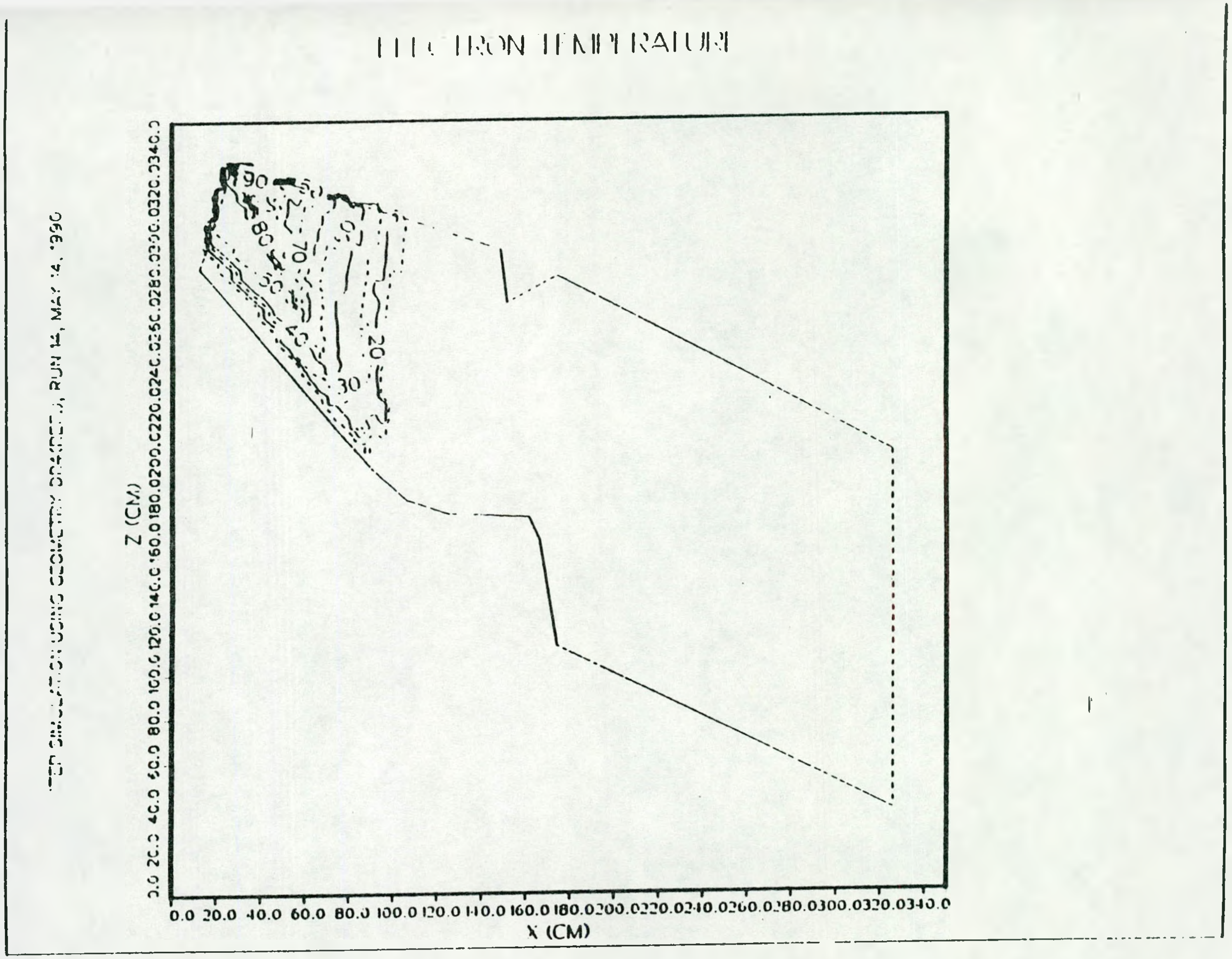


**Figure 2 b**

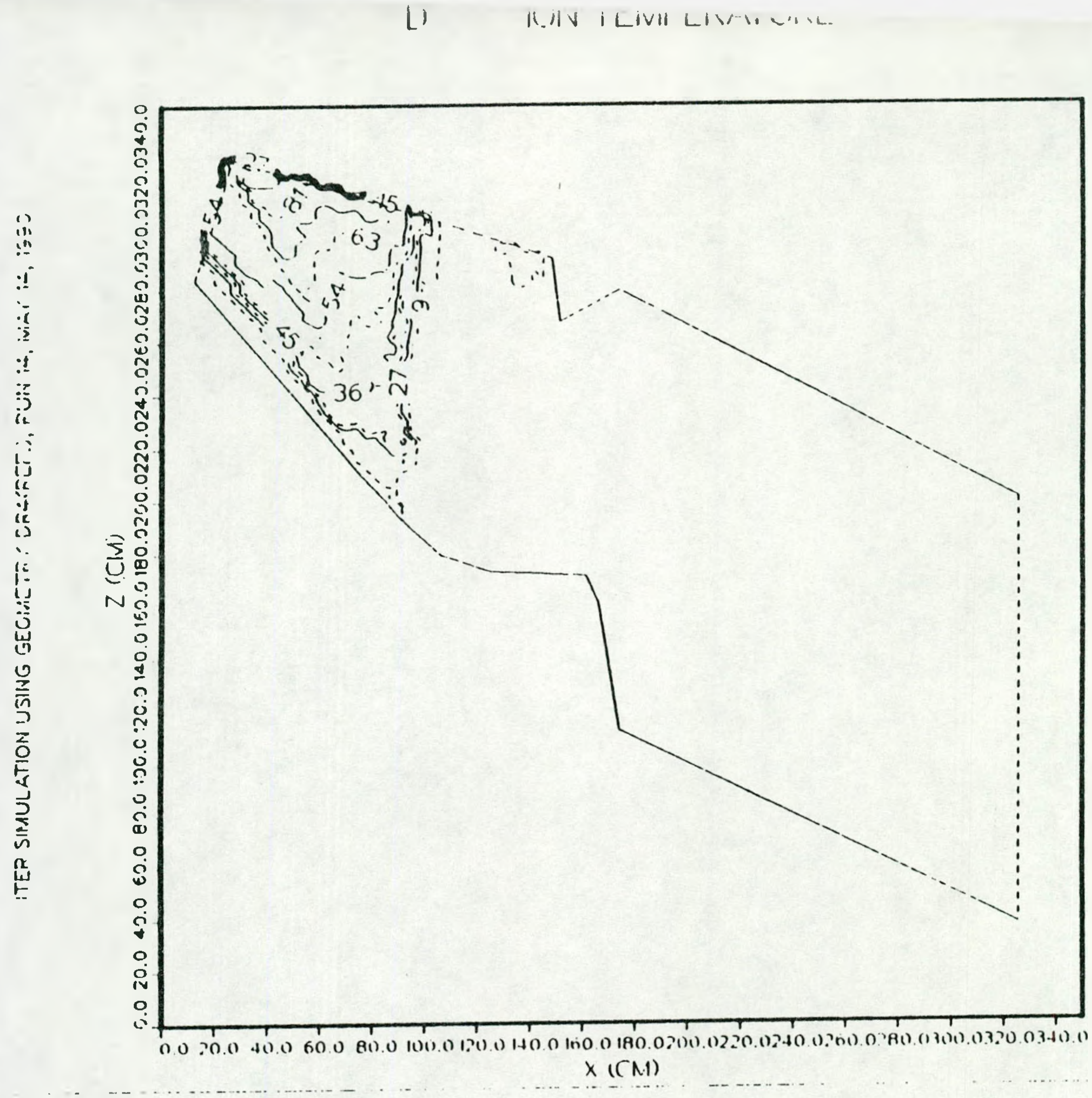


**Figure 2 c**

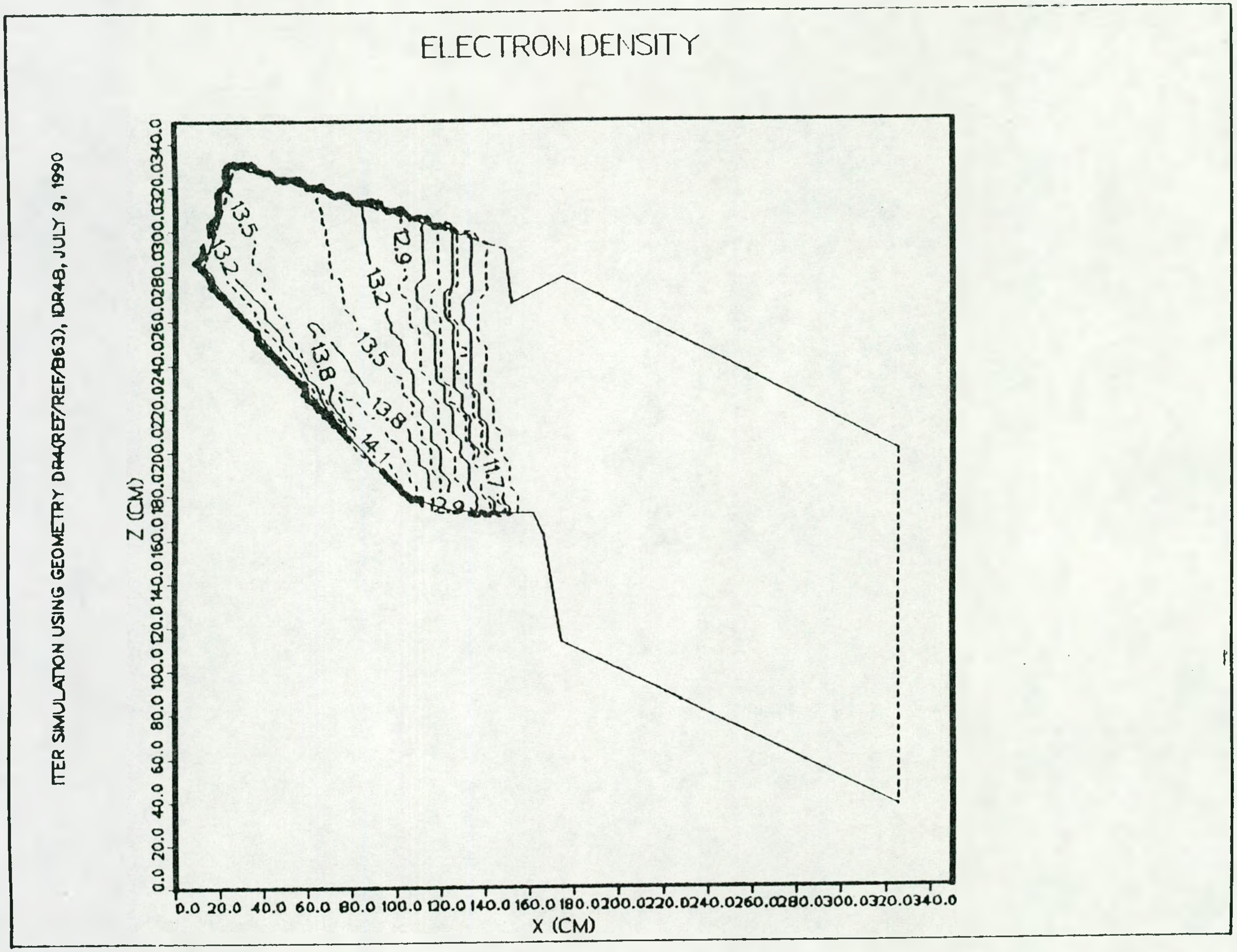

ELECTRON DENSITY
ITER SIMULATION USING GEOMETRY DR4(REF/REF/B63), IDR48, JULY 9, 1990
Z (CM)
X (CM)
0.0 20.0 40.0 60.0 80.0 100.0 120.0 140.0 160.0 180.0 200.0 220.0 240.0 260.0 280.0 300.0 320.0 340.0
13.5
13.2
12.9
13.2
13.5
13.8
13.8
14.1
11.7
12.9


Figure 2 d

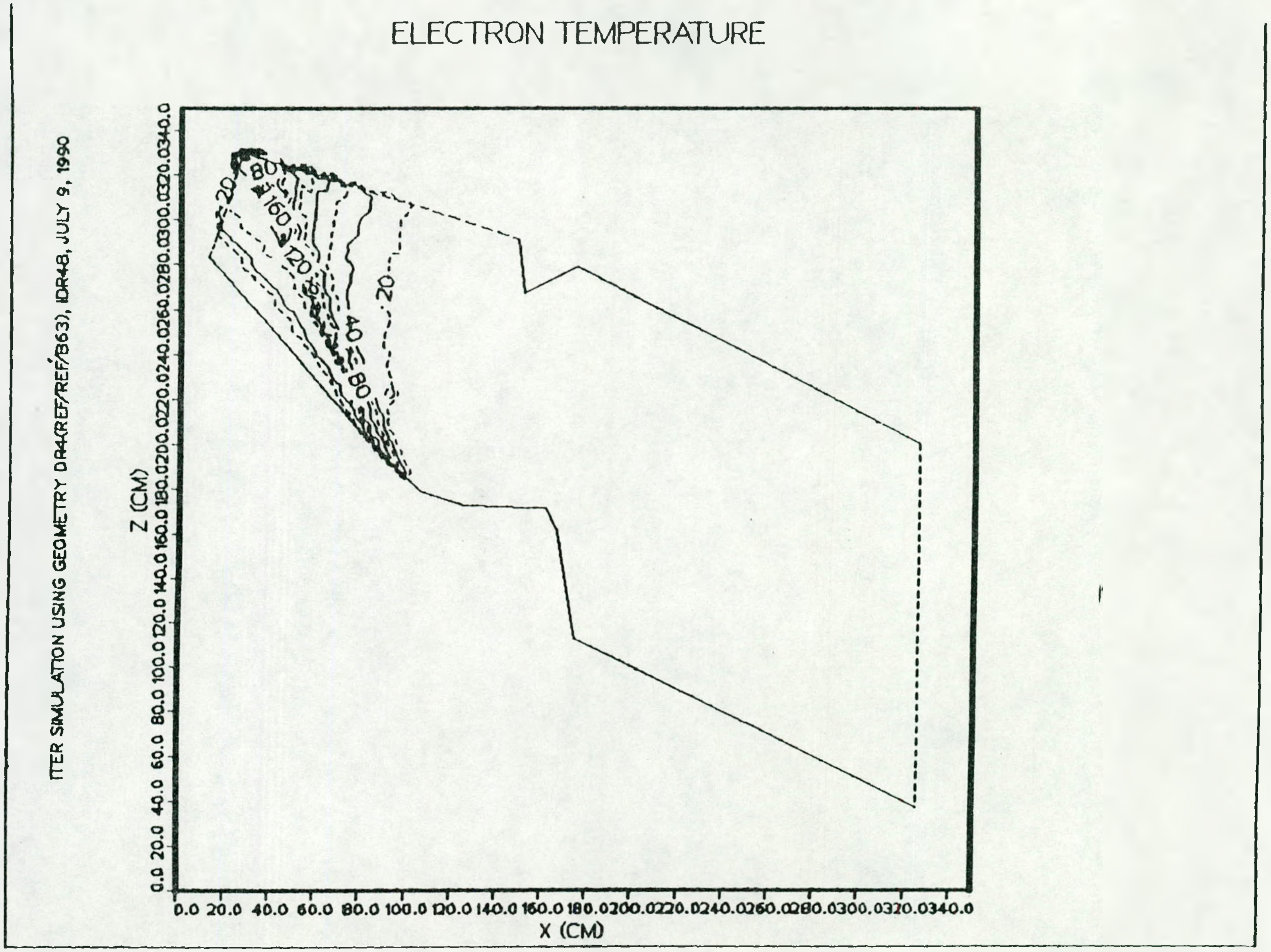

ELECTRON TEMPERATURE
ITER SIMULATION USING GEOMETRY DR4(REF/REF/B63), IDR48, JULY 9, 1990
Z (CM)
X (CM)
0.0 20.0 40.0 60.0 80.0 100.0 120.0 140.0 160.0 180.0 200.0 220.0 240.0 260.0 280.0 300.0 320.0 340.0
20
80
160
120
40
80
20


Figure 2 e

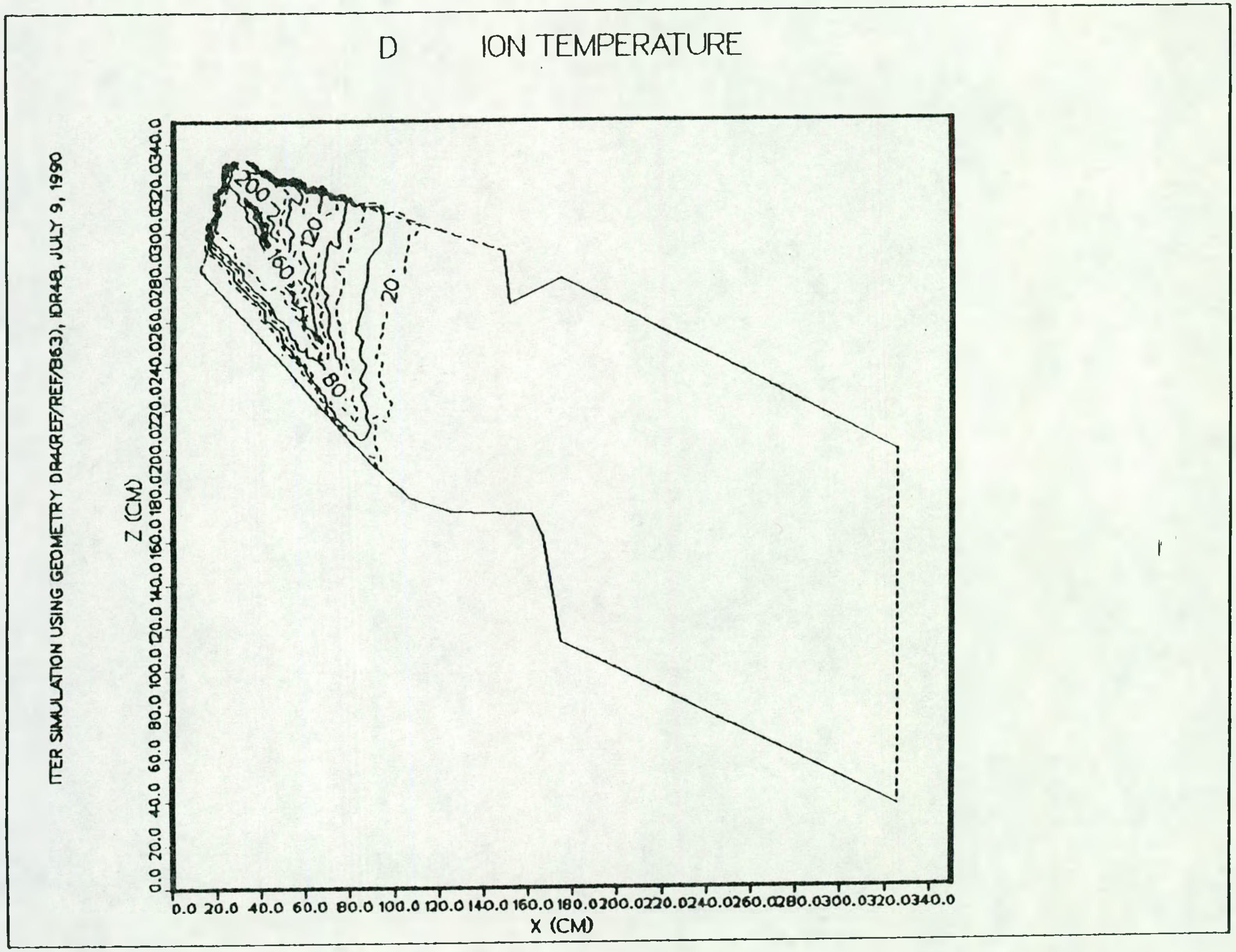
D
ION TEMPERATURE
ITER SIMULATION USING GEOMETRY DR4(REF/REF/B63), IDR48, JULY 9, 1990
Z (CM)
X (CM)
200
160
120
80
20
0.0 20.0 40.0 60.0 80.0 100.0 120.0 140.0 160.0 180.0 200.0 220.0 240.0 260.0 280.0 300.0 320.0 340.0

Fig. 2f

Flux Distribution Along Divertor Plate (reference case)

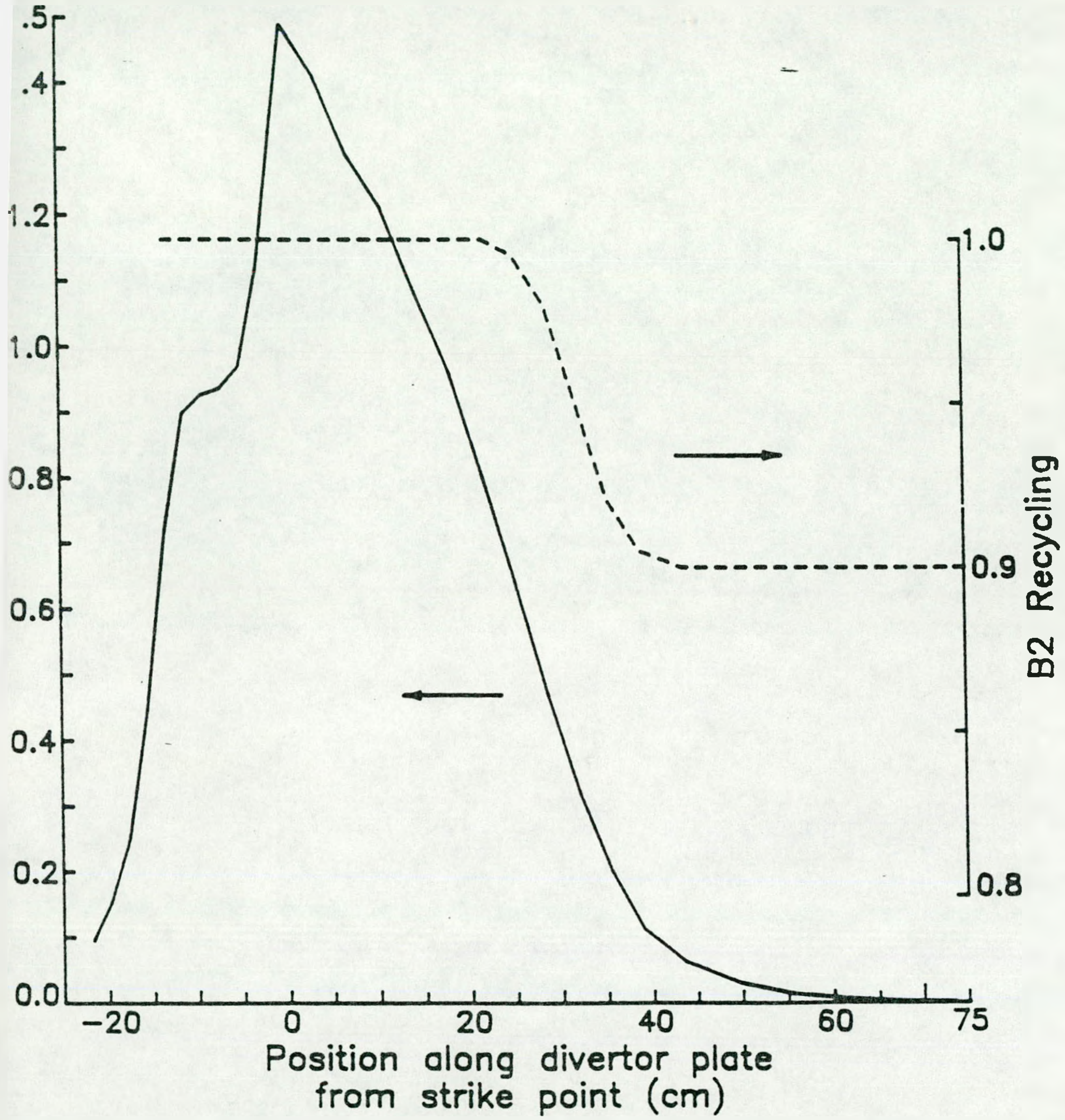


Figure 3

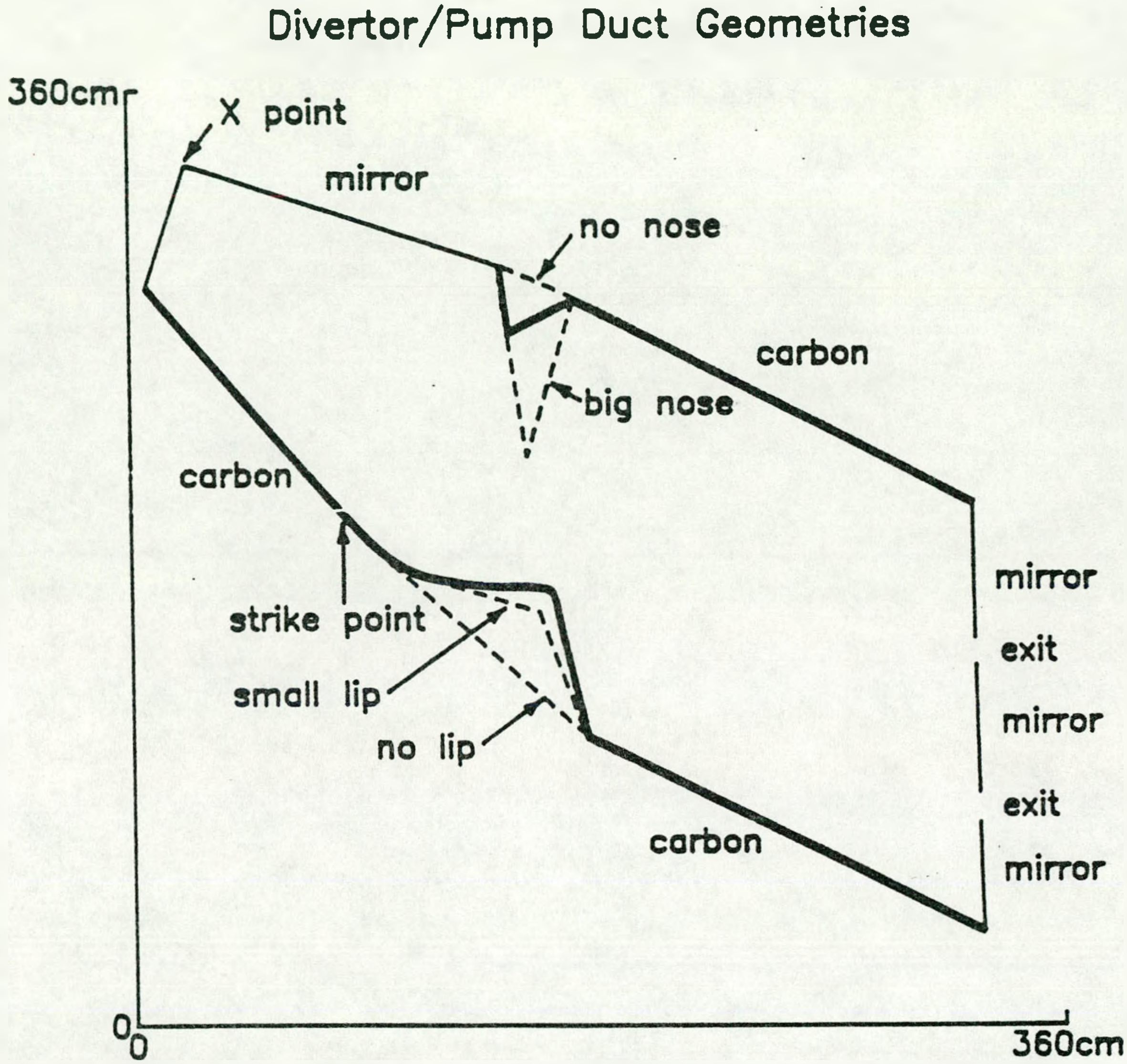
Divertor/Pump Duct Geometries
360cm
X point
mirror
no nose
carbon
big nose
carbon
mirror
strike point
exit
small lip
mirror
no lip
exit
carbon
mirror
0
0
360cm

Figure 4

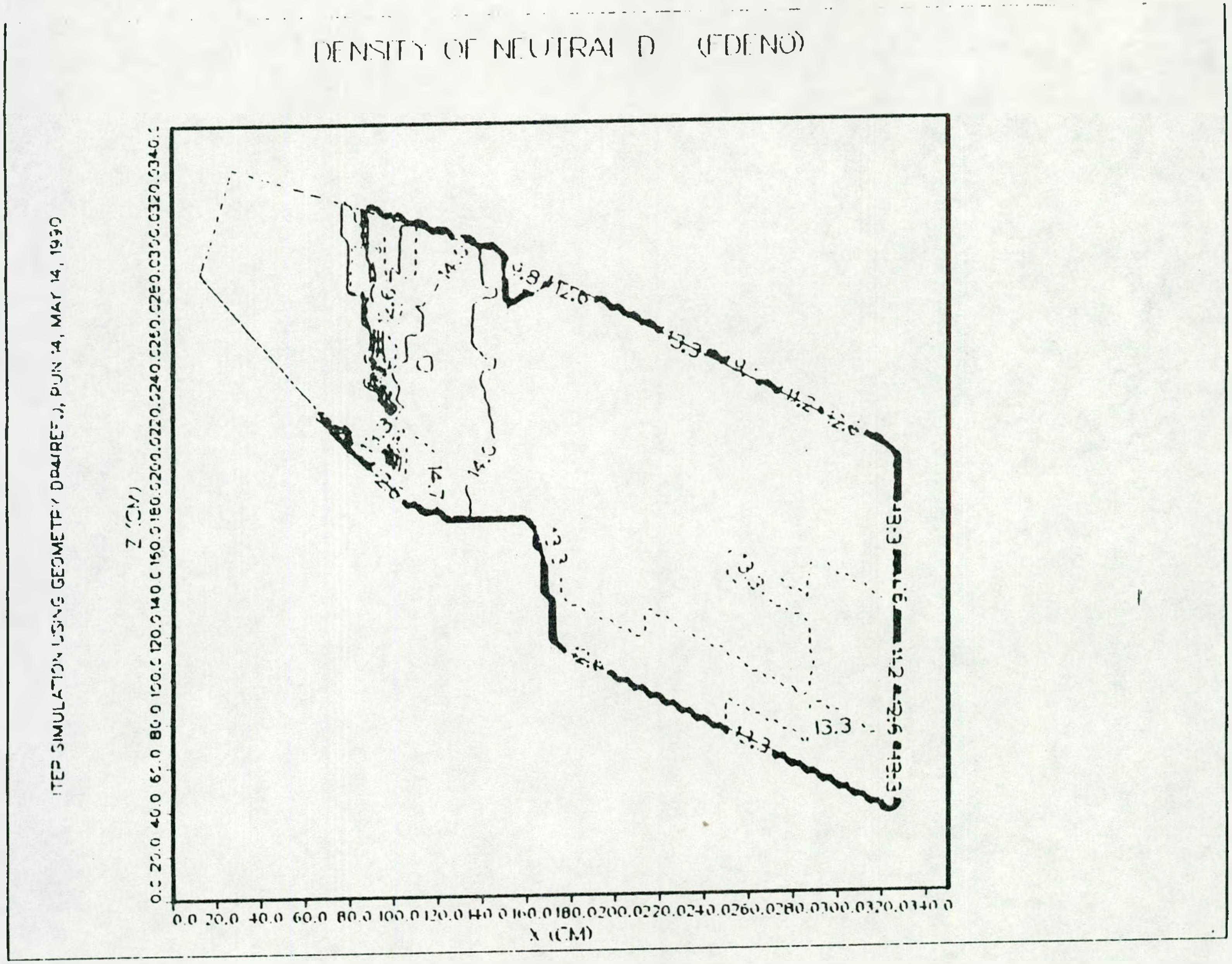


Figure 5 a

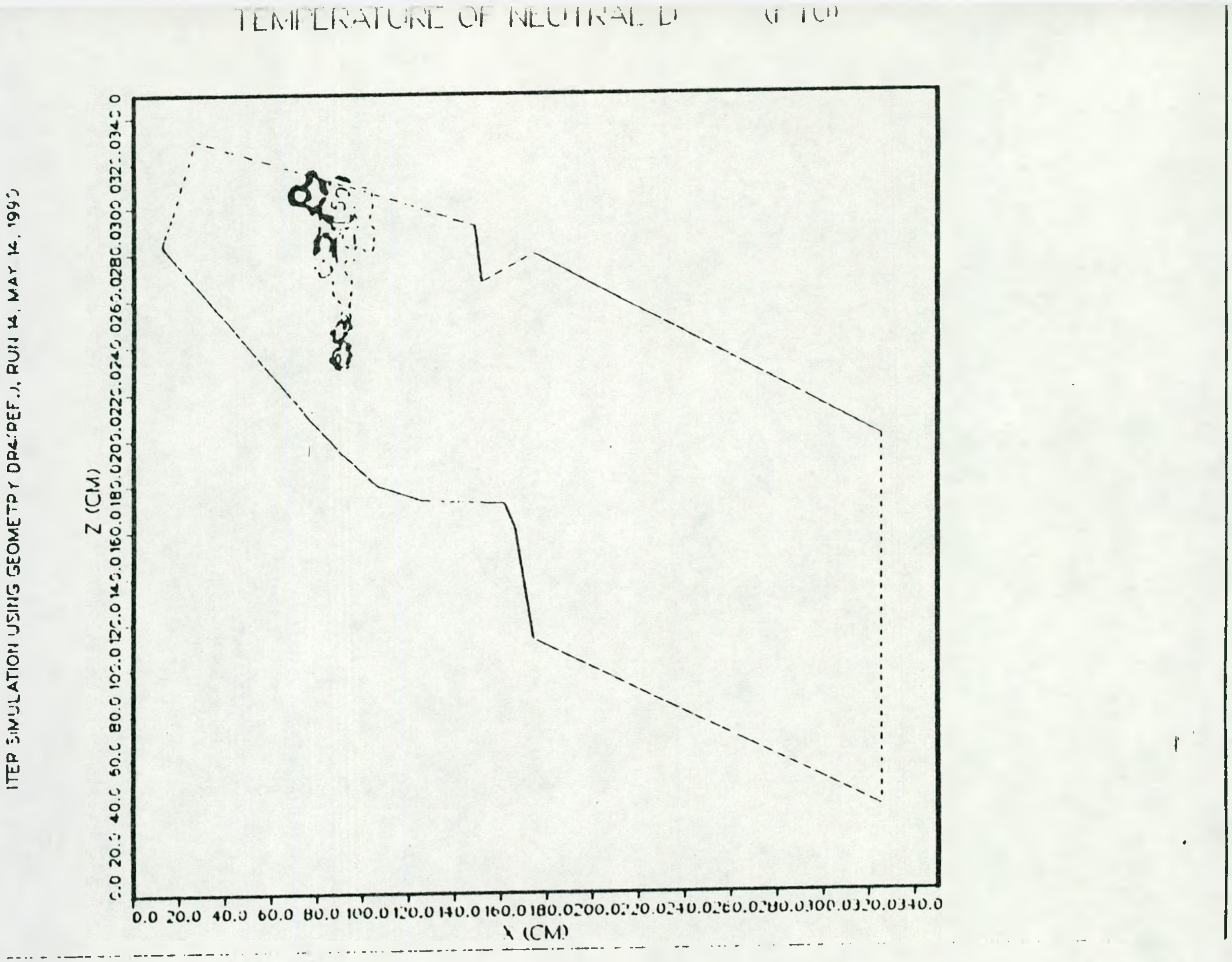


Figure 5 b

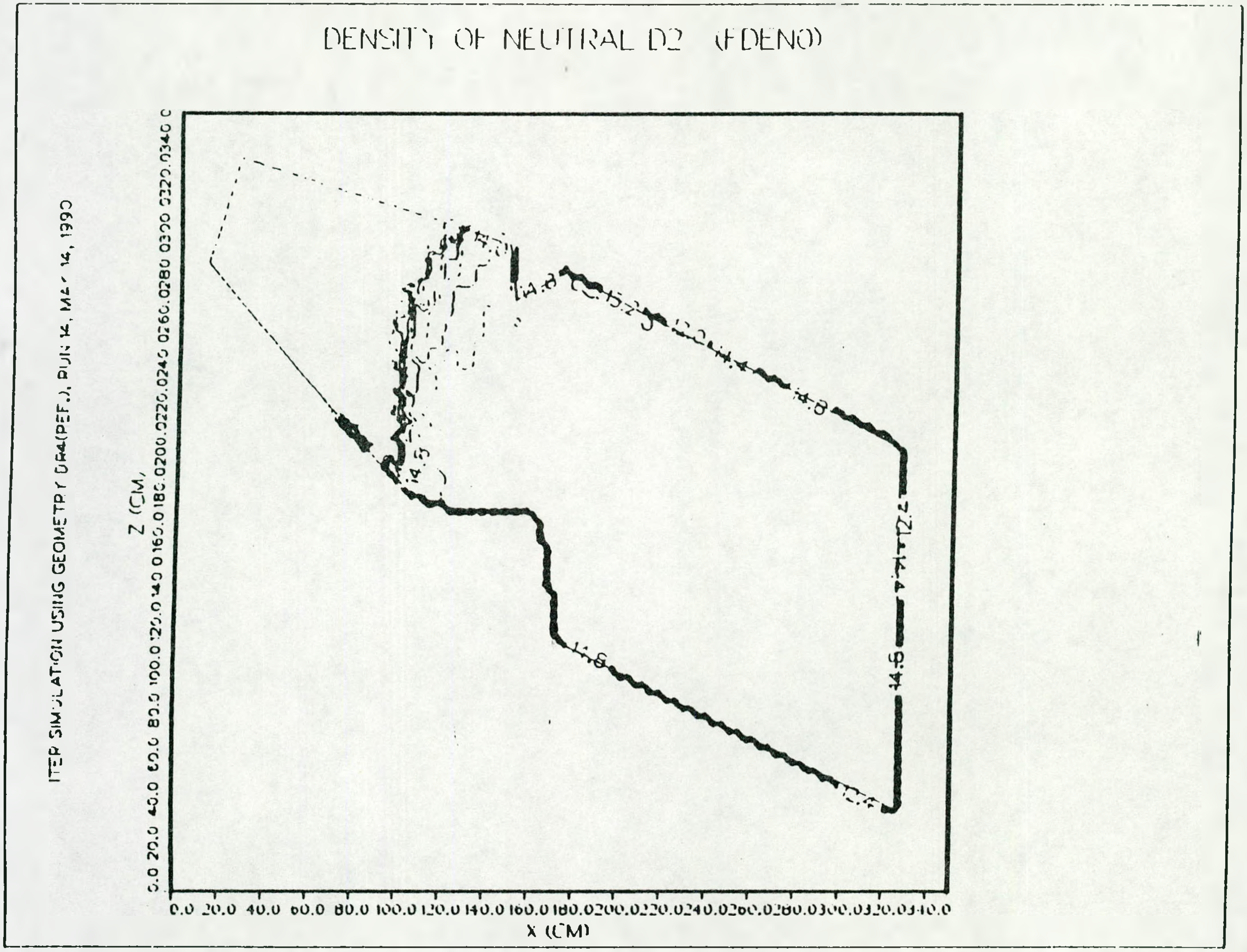
DENSITY OF NEUTRAL D2 (FDENO)
ITER SIMULATION USING GEOMETRY DR4(REF.), RUN 14, MAY 14, 1990
Z (CM)
X (CM)
0.0 20.0 40.0 60.0 80.0 100.0 120.0 140.0 160.0 180.0 200.0 220.0 240.0 260.0 280.0 300.0 320.0 340.0
14.8

**Figure 5 c**

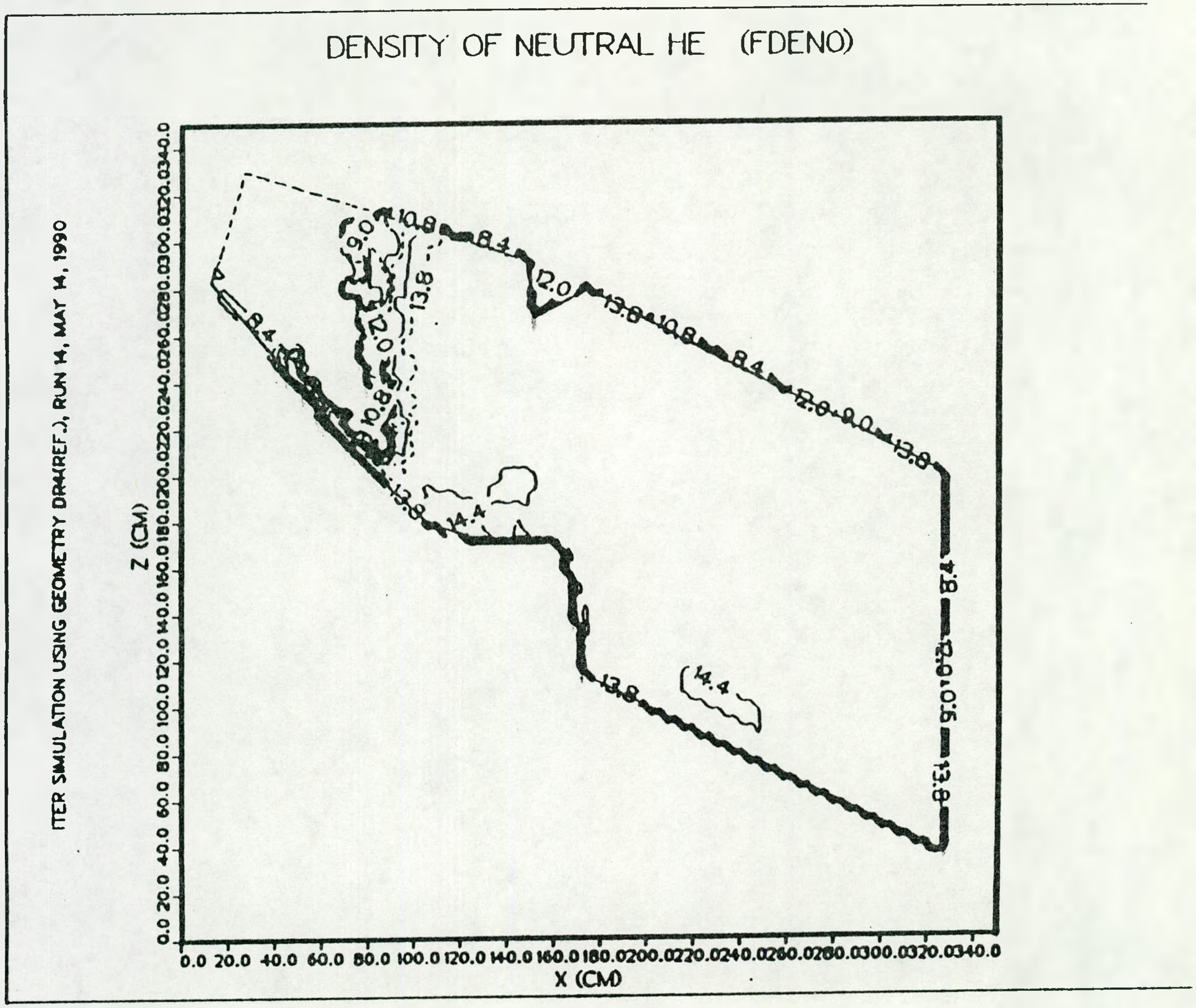

DENSITY OF NEUTRAL HE (FDENO)
ITER SIMULATION USING GEOMETRY DR4(REF.), RUN 14, MAY 14, 1990
Z (CM)
X (CM)


Figure 5 d

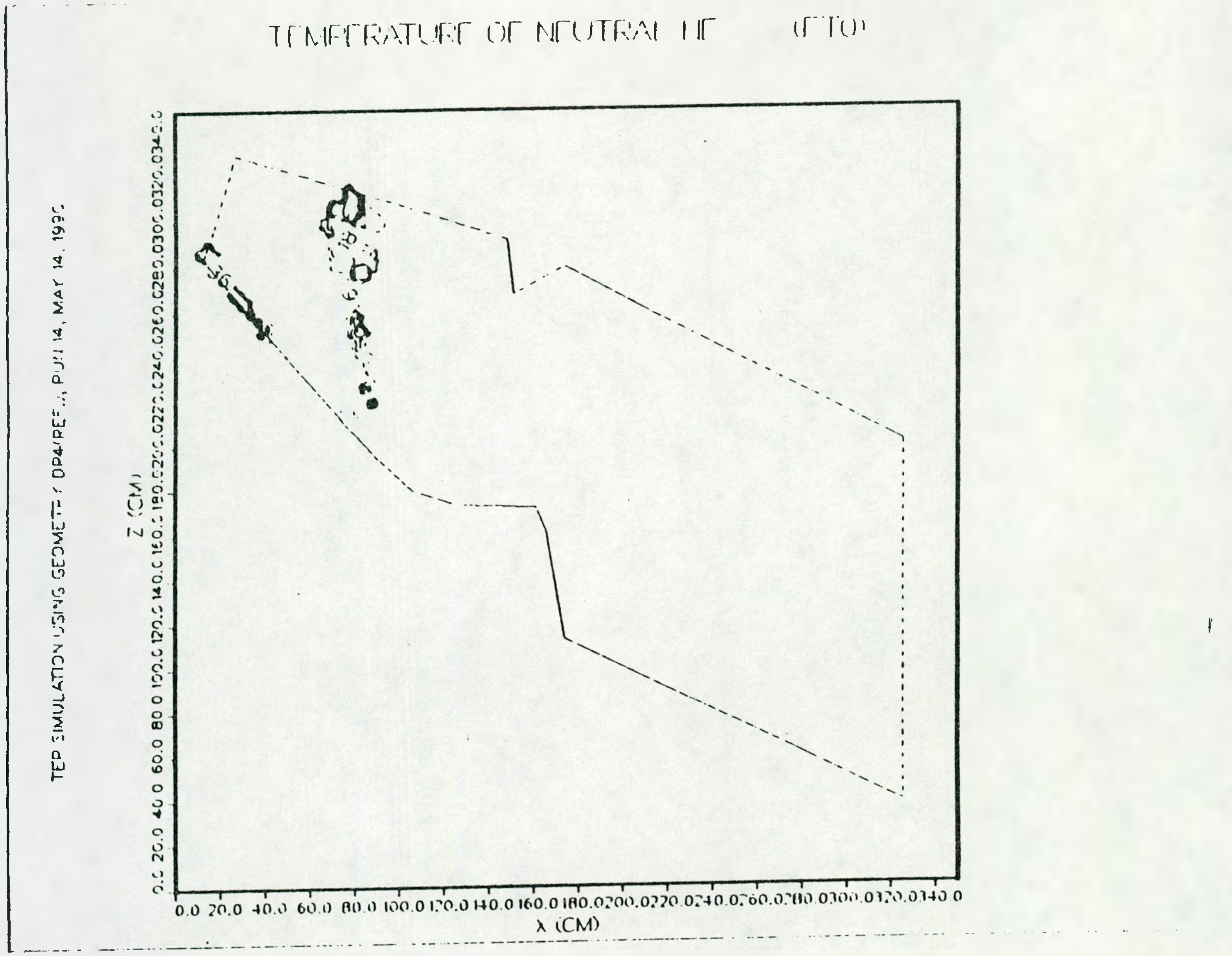
TEMPERATURE OF NEUTRAL HE (ETO)
TEP SIMULATION USING GEOMETRY DP4/PE..., RUN 14, MAY 14, 1993
Z (CM)
X (CM)
0.0 20.0 40.0 60.0 80.0 100.0 120.0 140.0 160.0 180.0 200.0 220.0 240.0 260.0 280.0 300.0 320.0 340.0

Figure 5 e

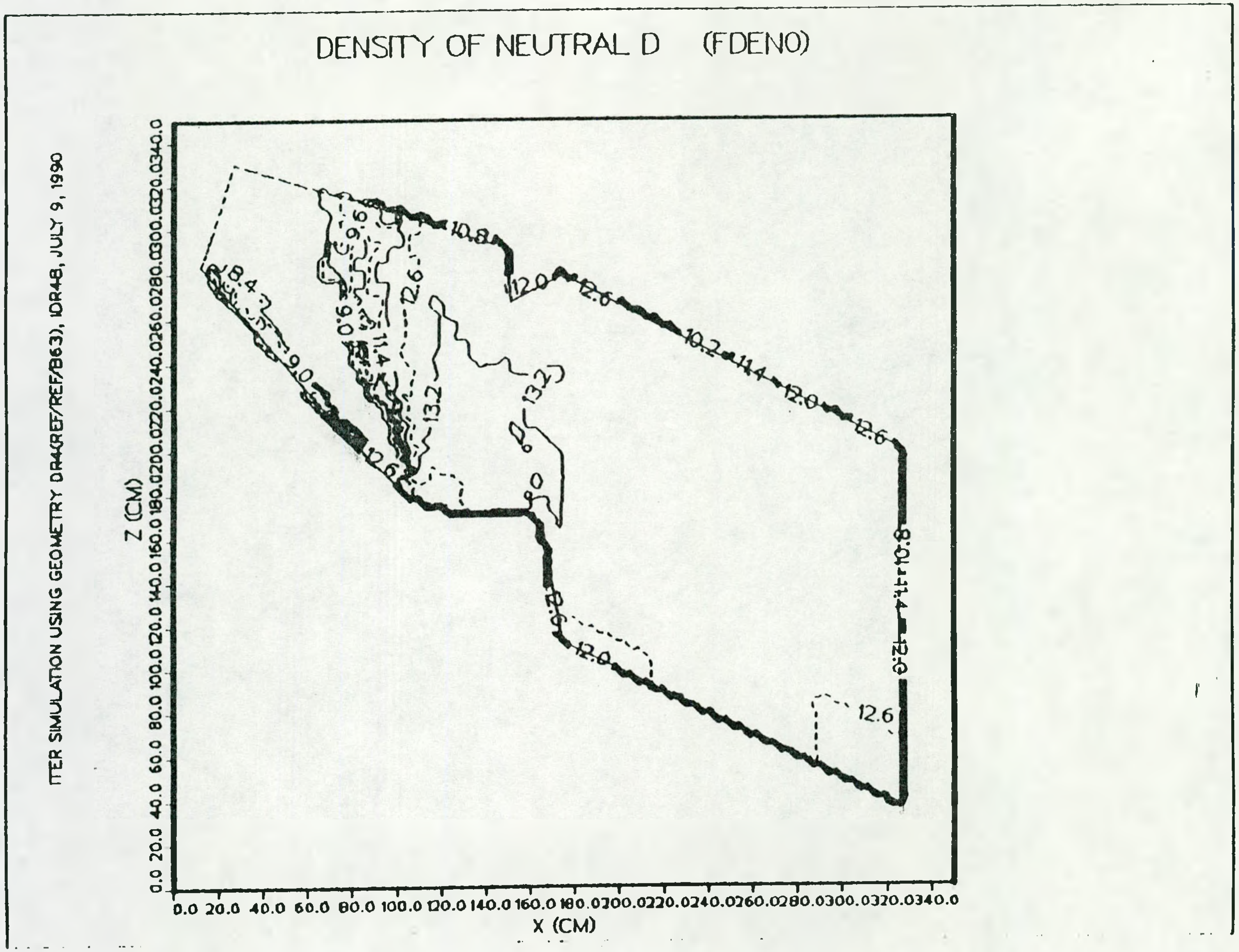
DENSITY OF NEUTRAL D (FDENO)
ITER SIMULATION USING GEOMETRY DR4(REF/REF/B63), IDR48, JULY 9, 1990
Z (CM)
0.0 20.0 40.0 60.0 80.0 100.0 120.0 140.0 160.0 180.0 200.0 220.0 240.0 260.0 280.0 300.0 320.0 340.0
X (CM)
0.0 20.0 40.0 60.0 80.0 100.0 120.0 140.0 160.0 180.0 200.0 220.0 240.0 260.0 280.0 300.0 320.0 340.0

Figure 5 f

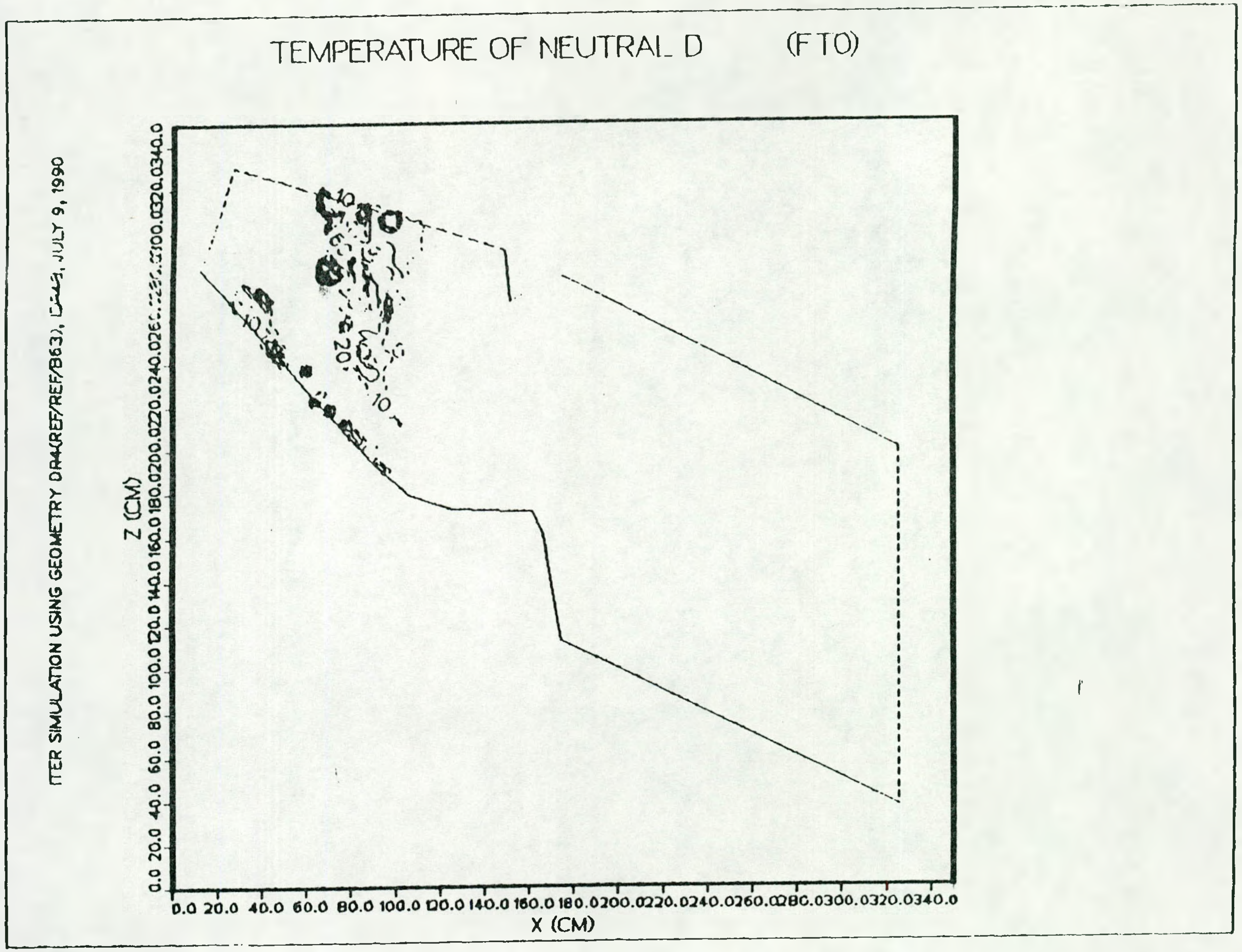
TEMPERATURE OF NEUTRAL D (FTO)
Z (CM)
X (CM)
0.0 20.0 40.0 60.0 80.0 100.0 120.0 140.0 160.0 180.0 200.0 220.0 240.0 260.0 280.0 300.0 320.0 340.0
10
20


Figure 5 g

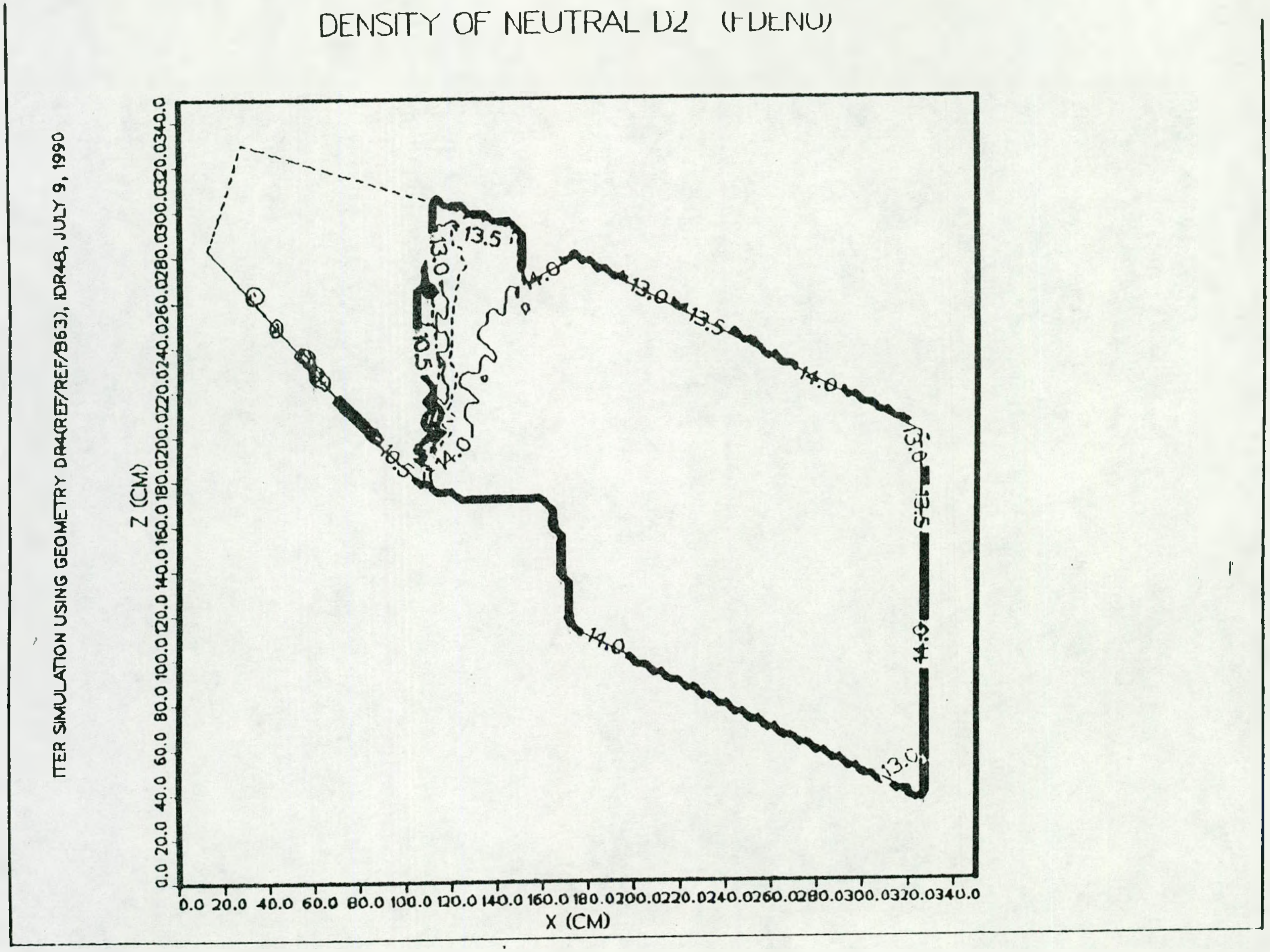
DENSITY OF NEUTRAL D2 (FDENO)
ITER SIMULATION USING GEOMETRY DR4(REF/REF/B63), IDR48, JULY 9, 1990
Z (CM)
X (CM)
13.5
13.0
14.0
10.5


Figure 5 h

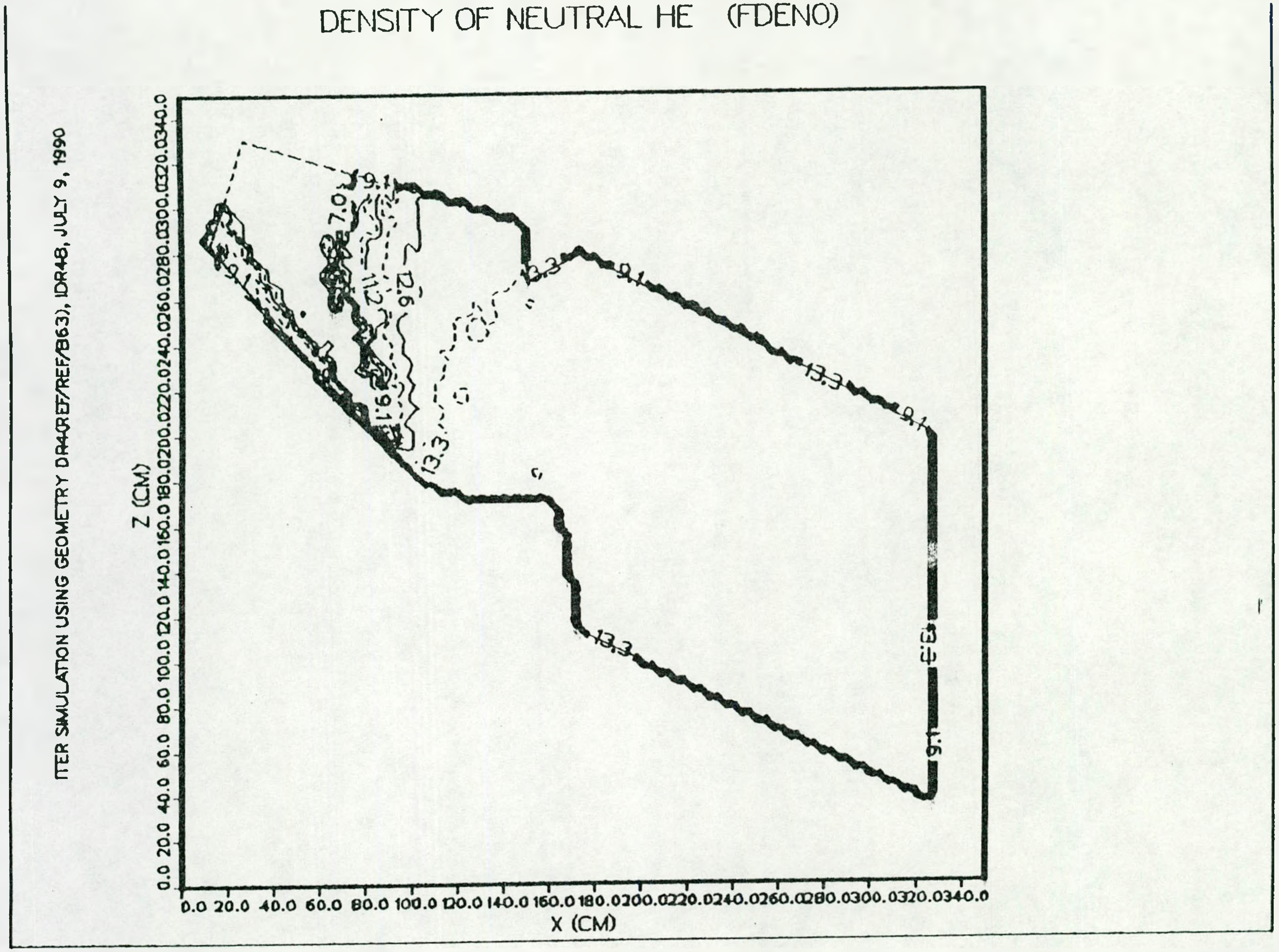
DENSITY OF NEUTRAL HE (FDENO)
ITER SIMULATION USING GEOMETRY DR4(REF/REF/B63), IDR48, JULY 9, 1990
Z (CM)
X (CM)
0.0 20.0 40.0 60.0 80.0 100.0 120.0 140.0 160.0 180.0 200.0 220.0 240.0 260.0 280.0 300.0 320.0 340.0
9.1
7.0
12.6
11.2
13.3

Figure 5 i

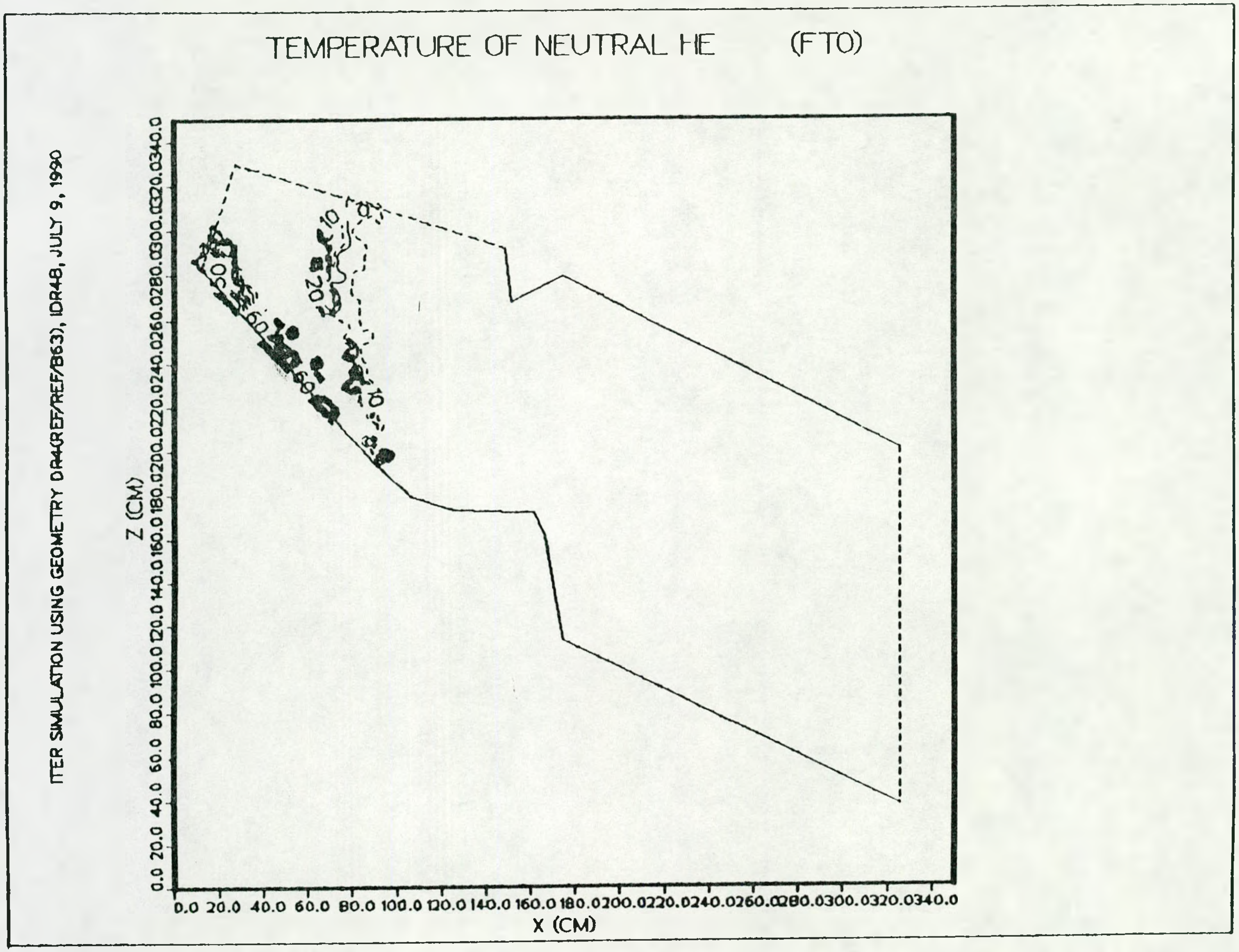
TEMPERATURE OF NEUTRAL HE (FTO)
ITER SIMULATION USING GEOMETRY DR4(REF/REF/B63), IDR48, JULY 9, 1990
Z (CM)
X (CM)
0.0 20.0 40.0 60.0 80.0 100.0 120.0 140.0 160.0 180.0 200.0 220.0 240.0 260.0 280.0 300.0 320.0 340.0
10
20
50
60
10

Figure 5 j

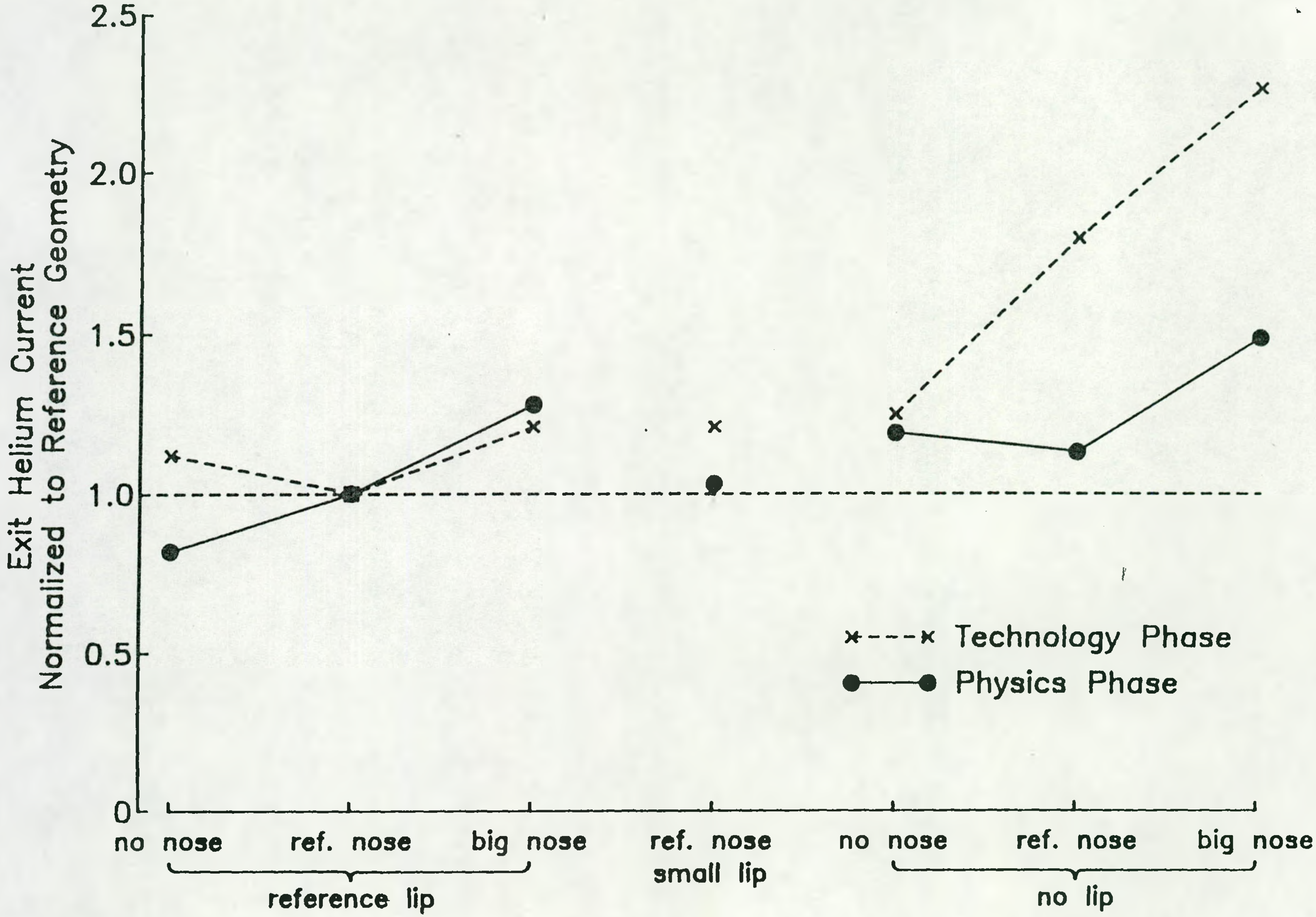
Exit Helium Current
Normalized to Reference Geometry
2.5
2.0
1.5
1.0
0.5
0
Technology Phase
Physics Phase
no nose
ref. nose
big nose
reference lip
ref. nose
small lip
no nose
ref. nose
big nose
no lip

Figure 6

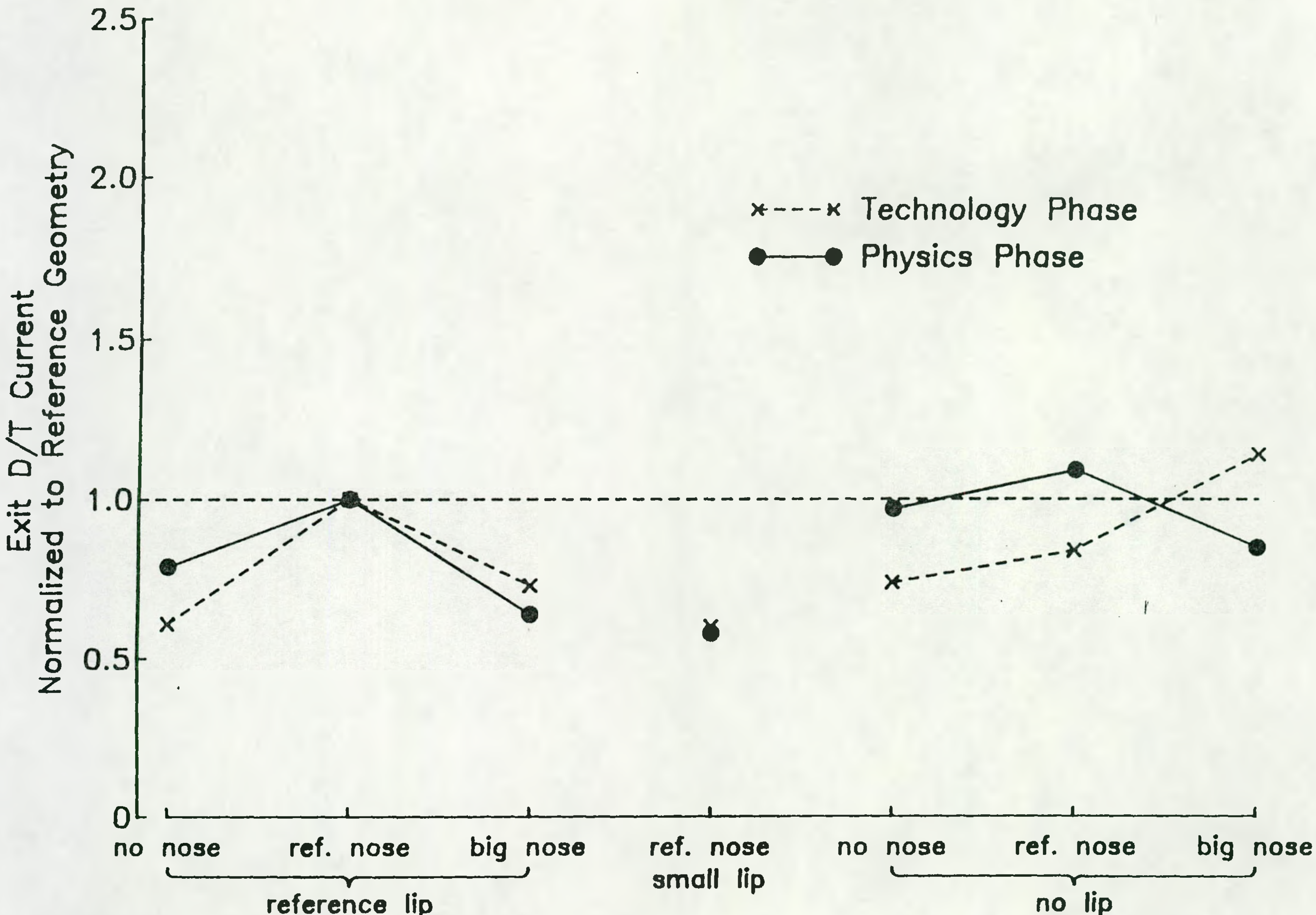
Exit D/T Current
Normalized to Reference Geometry
2.5
2.0
1.5
1.0
0.5
0
Technology Phase
Physics Phase
no nose
ref. nose
big nose
reference lip
ref. nose
small lip
no nose
ref. nose
big nose
no lip

Figure 7

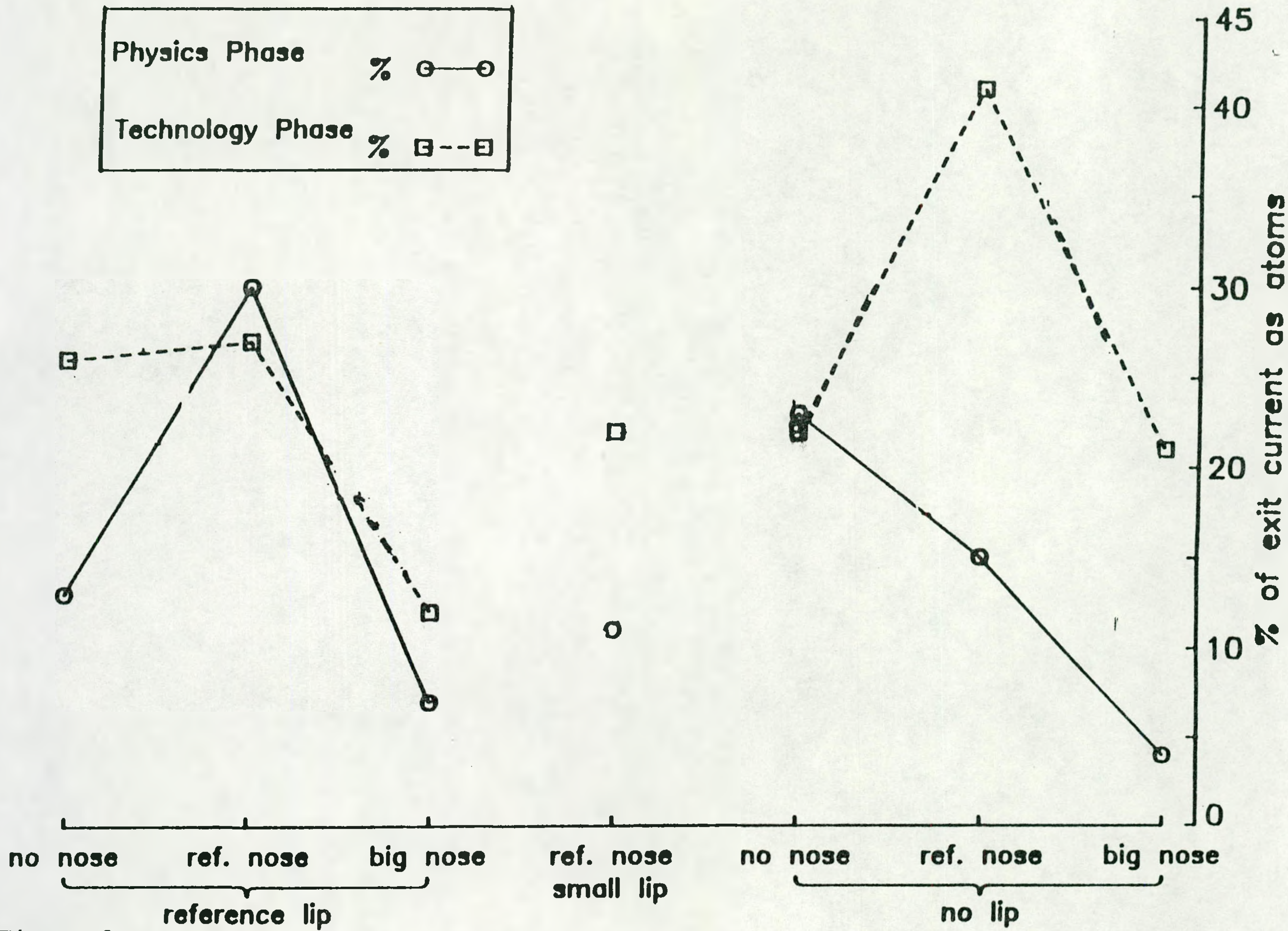
Physics Phase %
Technology Phase %
45
40
30
20
10
0
% of exit current as atoms
no nose
ref. nose
big nose
ref. nose
small lip
no nose
ref. nose
big nose
reference lip
no lip

Figure 8

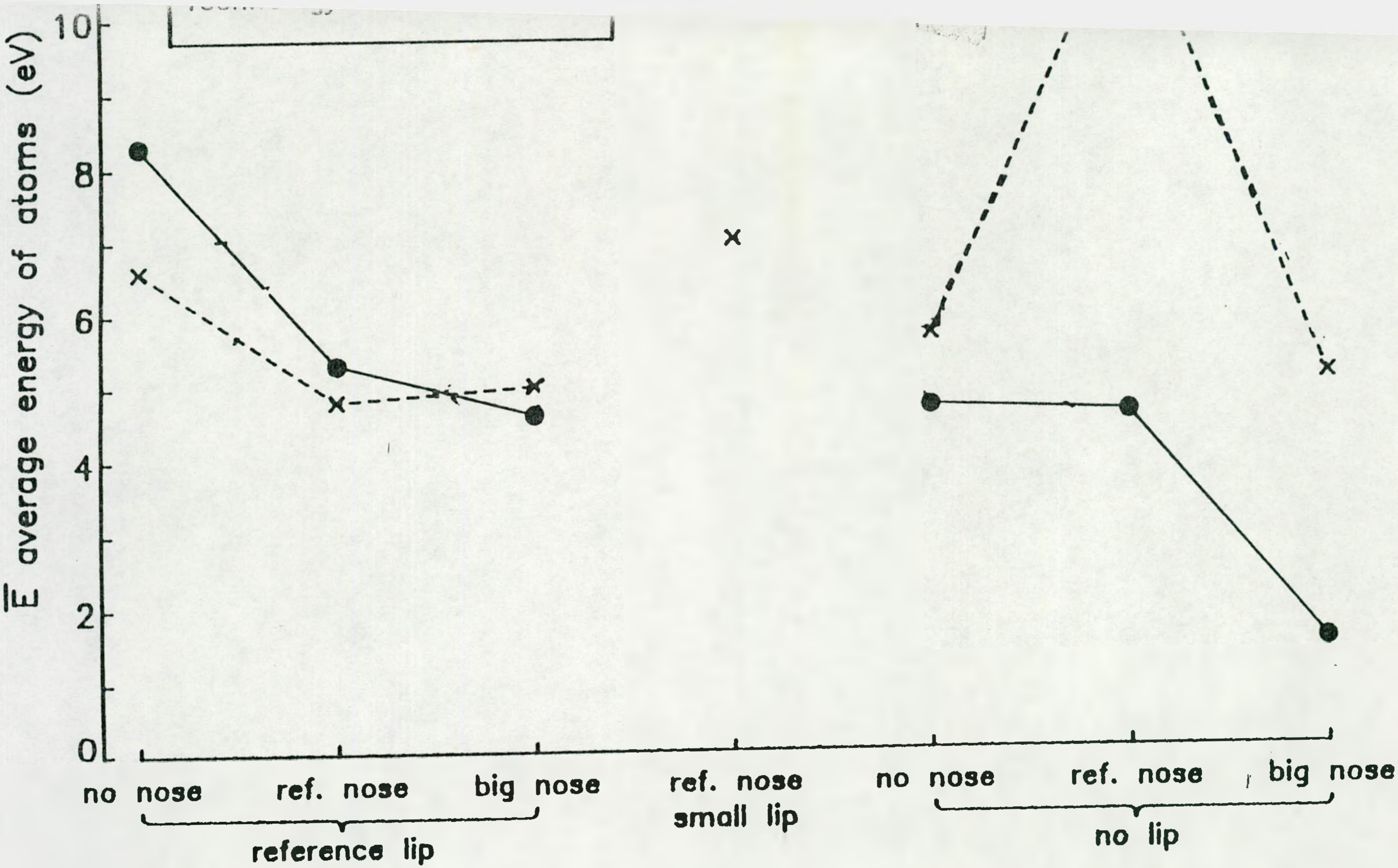

10
8
6
4
2
0
$\overline{E}$ average energy of atoms (eV)
no nose
ref. nose
big nose
reference lip
ref. nose
small lip
no nose
ref. nose
big nose
no lip


Figure 9